Universidade do Minho
Escola de Ciências

Juliana Justino de Andrade

Self-assembled noncovalent hydrogels based on dehydrodipeptides

October of 2012

Juliana Justino de Andrade **Self-assembled noncovalent hydrogels based on dehydrodipeptides**

UMinho | 2012

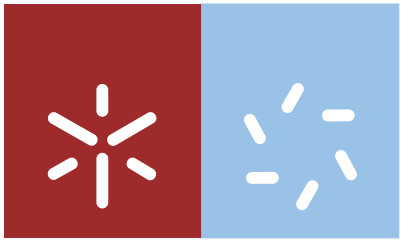

Universidade do Minho
Escola de Ciências

Juliana Justino de Andrade

Self-assembled noncovalent hydrogels based on dehydrodipeptides

Master dissertation in Medicinal Chemistry

This work was accomplished under the supervision of:
Paula Margarida Vidigal Soares Teixeira Ferreira
José Alberto Ribeiro Martins

October of 2012

Autora:

Juliana Justino de Andrade

E-mail: juliana.j.andrade@gmail.com

Dissertação de Mestrado em Ciências. Área de Conhecimento: Química Medicinal.

Título: Hidrogéis preparados a partir da automontagem de desidrodipéptidos.

Ano de Publicação: 2012.

Orientadores:

Paula Margarida Vidigal Soares Teixeira Ferreira.

José Alberto Ribeiro Martins.

This work was supported by:

FCT
Fundação para a Ciência e a Tecnologia
MINISTÉRIO DA CIÊNCIA, TECNOLOGIA E ENSINO SUPERIOR

EMUNDUS17
ERASMUS MUNDUS EXTERNAL COOPERATION WINDOW / LOTE 17

“A felicidade aparece para aqueles que choram. Para aqueles que se machucam. Para aqueles que buscam e tentam sempre. E para aqueles que reconhecem a importância das pessoas que passam por suas vidas.”

Clarice Lispector

Acknowledgements

I would like to thank my supervisors Paula Margarida Ferreira and José Alberto Martins for all the support during the development of this work. I definitely will keep a special place for them in my heart and will remember all the lessons taught by them.

I am grateful to the Chemistry Department and Chemistry Center of the University of Minho for providing the technical and human conditions that made this work possible.

I take special pleasure in acknowledge Professor Rui Brito from the Department of Chemistry, University of Coimbra, for providing the conditions for the CD study.

I really owe sincere thankfulness to my laboratory colleagues Goreti and Helena who helped me with important discussions about the work and with some procedures that were crucial for having all work done successfully.

To my department friends Janaina, Alexandra, Raquel, Gonçalo and António I offer my gratitude for all special moments spent together and for receiving me open heartily during my mobility. These fellows really made it easier to accomplish this work and gave me courage to overcome difficulties.

I am truly indebted and thankful to my special friends Ana Luisa Rodrigues and Jorge Manuel Ferreira that were like rocks to me and with whom I could count during all my stay in Portugal. They are angels that appeared to light my way and to make my journey less arduous.

Finally, but not less relevant, I would like to thank my parents, my sister, my family and brazilian friends that always believed me and gave all the love and strength I needed to carry on following my dreams, mainly in the most difficult moments.

Abstract

Self-assembly of nanometric structures from molecular building blocks is an effective way to make new functional materials for biological and technological applications.

In this work we synthesized new N-modified dehydrodipeptides based on phenylalanine and dehydroamino acid units attached to aromatic modifiers, namely trimesoyl, terephtaloyl, diphenylacetyl and 2,2´-(1,3-phenylene)diacetyl in a pattern that afforded mono or polysubstitued organic molecules. The potential use of these new compounds as hydrogelators was evaluated. The results showed that most of the prepared compounds behave as efficient molecular hydrogelators forming hydrogels at minimum gelation concentrations of 0.3-0.8 wt%.

Two new compounds failed to form hydrogels probably due to unfavorable thermodynamic contribution of intermolecular interactions.

The self-aggregation pattern of the hydrogelators was investigated by STEM microscopy technique, revealing different shapes depending on the N-aromatic moiety. A circular dichroism analysis was also performed in order to evaluate if the peptides aggregate into any characteristic secondary structure, usually found in protein folding. We found that the 5 hydrogelators had characteristic signals, demonstrating the presence of organized structures even below the minimum gelation concentration. At elevated pH or for the non-hydrogelating compounds, it was not observed signals indicative of the presence of such structures.

Keywords: hydrogels; hydrogelators; dehydrodipeptides; dehydroamino acids.

Resumo

A automontagem de estruturas manométricas, a partir de entes de dimensão molecular, consiste em uma alternativa eficiente para a síntese de novos materiais funcionais para aplicações biotecnológicas.

Neste trabalho, foram sintetizados novos desidrodipéptidos modificados em sua porção N-terminal. Os dipéptidos continham fenilalanina e desidroaminoácidos e os grupos modificadores foram grupos aromáticos (trimesoil, tereftaloil, difenilacetil e o 2,2´-(1,3-phenileno)diacetil) os quais foram conjugados de forma a gerar compostos mono ou polissubstituídos. A capacidade de gelificar em meio aquoso, destes novos compostos, foi avaliada e os resultados mostraram que a maioria deles conseguiram gelificar em meio aquoso em concentrações mínimas na faixa 0.3-0.8 m%.

Dois destes compostos não conseguiram originar hidrogéis, provavelmente devido a um balanço termodinamicamente desfavorável das interacções intermoleculares entre os constituintes do sistema.

O padrão morfológico resultante da auto-agregação dos compostos que geraram os hidrogéis foi investigado pela técnica de microscopia electrónica de transmissão por scaneamento (STEM). Esta análise revelou que houve a ocorrência de diferentes tipos de estruturas nos hidrogéis, dependendo de qual modificador aromático foi utilizado.

Também realizou-se uma análise de Dicroísmo Circular para avaliar se os péptidos agregavam-se em algum padrão de estrutura secundária característica de enovelamento proteico. Detectou-se que nos 5 agentes gelificates haviam sinais característicos da presença de estruturas organizadas mesmo abaixo da concentração de gelificação mínima. Em pH elevado e nas moléculas não gelificantes, não se observam sinais indicativos da presença deste tipo de estruturas.

Palavras-chave: hidrogéis; desidro-aminoácidos; desidrodipéptidos.

Table of contents

List of Abbreviations and Symbols

%	Percentage
°C	Celsius degrees
2D	Bidimensional
3D	Tridimensional
aa	Amino acid
Abs	Absorvance
Abu	Aminobutyric acid
ACN	Acetonitrile
Ar	Aromatic
Boc	*tert*-butylcarbonyl
Boc_2O	Di-*tert*-butyl dicarbonate
br. s	broad singlet
CD	circular dichroism
$CDCl_3$	Deuterated chloroform
cgc	Critical gelation concentration
CH_2Cl_2	Dichloromethane
d	Doublet
DCC	Dicyclohexylcarbodiimide
dd	double doublet
DHD	Dehydrodipeptide
DMAP	4-dimethylaminopyridine
DMF	Dimethylformamide
DMSO-d^6	deuterated dimethylsulfoxide
Fmoc	9-fluorenylmethoxycarbonyl
g	Grams
G´	storage modulus
G´´	loss modulus
Gly	Glycine
h	Hours
HMBC	Heteronuclear Multiple Bond Coherence
HOBt	Hydroxybenzotriazole
HSQC	Heteronuclear Multiple Quantum Coherence
Hz	Hertz
J	coupling constant
LMWGs	Low molecular weight gelators
m	Multiplet
m	*Meta*
M	Molar (mmol/mL)
m.p.	melting point

mg	Miligrams
MHz	Megahetz
min	Minutes
mL	Mililitre
mmol	Milimol
Nap	Naphtalene
NHS	N-hydroxysucinimide
nm	Nanometer
NMR	Nuclear magnetic resonance
^{13}C-NMR	Nuclear magnetic resonance of ^{13}C
^{1}H-NMR	Nuclear magnetic resonance of ^{1}H
o	*Ortho*
p	*Para*
pH	Hydrogenionic potencial
Phe	Phenylalanine
ppm	Parts per million
q	Quartet
r.t.	Room temperature
s	Singlet
STEM	Scanning electron microscopy
t	Triplet
TEA	Triethylamine
TFA	trifluoracetic acid
THF	Tetrahydrofurane
Thr	Threonine
t.l.c	Thin layer chromatography
TMG	N,N,N,N' – tetramethylguanidine
UV	Ultraviolet
Val	Valine
δ	Chemical shift
ΔAbu	Dehydroaminobutyric acid
ΔPhe	Dehydrophenylalanine
μm	Micrometer

List of Illustrations

List of tables

1. Introduction

The search for new self-assembling low molecular weight hydrogelators is attracting an increasing interest of the scientific society[1]. Searching the web of science data base, with the topic "Self-Assembled Low Molecular Weight Hydrogels" reveals that the number of citations is getting higher over the years (Figure 1). This can be ascribed mainly to the versatility of these materials for biomedical purposes owing to their rapid response to external stimuli, thermoreversible nature, and potential biodegradability[2, 3].

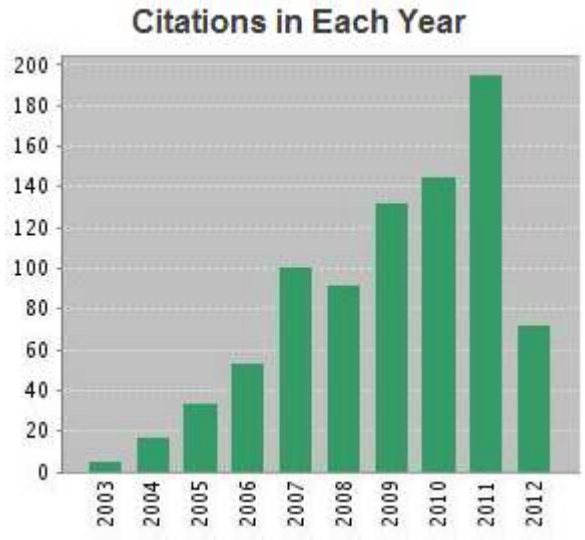

Figure 1 Data retrieved from Web of science with the search "Self-Assembled Low Molecular Weight Hydrogels" - until June of 2012.

1.1. Gels and Hydrogels

According to Almdal *et al*[4] a gel is a soft solid or solid-like colloidal system composed of a solid dispersed in a liquid. From the rheology point of view, gels can be characterized by a well-pronounced plateau in G'(ω) with G'(ω) > G"(ω) in a wide range of frequencies. Besides this, the transition of the gel material to a liquid behavior must occur at sufficiently low frequencies, i.e. when the longest relaxation time is, at least, in the order of seconds. This behavior is observed in Figure 2 for a polymeric gel material:

this material enters the terminal zone, i.e the region characteristic of the liquid-like behavior, at angular frequencies less than 10^{-3} rad/s, which corresponds to a terminal relaxation time in the order of 10^3 s; in this polymer, G'(ω) exhibits a plateau extending to frequencies lower than 1 rad/s, i.e. times longer than 1 s, and G'(ω) is much larger than G"(ω).

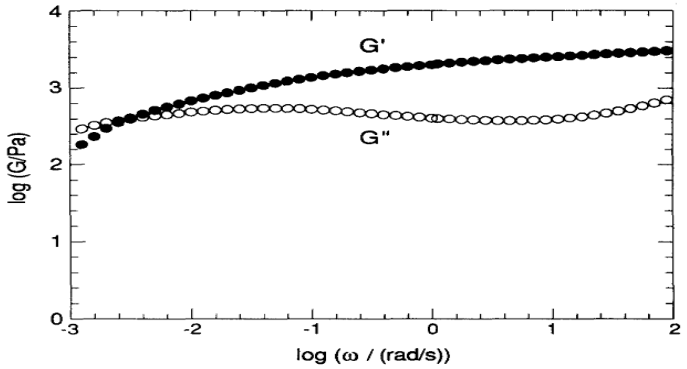

Figure 2 Log-log plot of storage modulus, G'(ω), and loss modulus, G"(ω), *versus* angular frequency for a 13.9% (w/w) solution of polystyrene in di(2-ethylhexyl) phthalate[4].

One specific type of gel are the **hydrogels**, which are soft materials composed of a three dimensional scaffold made of a hydrophilic network, capable of encapsulating water molecules, and retaining a large amount of fluids in the swollen state[4]. Their ability to absorb water is attributed to the presence of hydrophilic functional groups such as –OH, –CONH–, $–CONH_2–$, and $–SO_3H$ in polymers forming hydrogel structures[5].

1.2. Classification of hydrogels

Generally speaking, hydrogels can be classified taking into account many aspects, such as the nature of side groups (neutral or ionic), mechanical features, manufacture process (homopolymerization or co-polymerization), physical structure (amorphous, semicrystalline, hydrogen bonded, supramolecular and hydrocolloidal) and responsiveness to physiologic environment stimuli (pH, ionic strength, temperature, electromagnetic radiation, etc.).[6,7]

Based on the macromolecular architecture of the gel network, hydrogels can be divided into **covalent** or **noncovalent** hydrogels:

a) Covalent hydrogels or chemically cross-linked hydrogels are formed due to reticulation of hydrophilic polymers or by the irreversible cross-linking of the polymeric structure through covalent bonds. These links result from chemical or photo-initiated polymerization, disulfide bond formation, catalyzed metathesis or other chemical reaction[8,9].

b) Noncovalent hydrogels or physically cross-linked hydrogels are composed most frequently of ribbons, fibers and tubules that aggregate by anisotropic self-assembly of structures guided by noncovalent inter or intramolecular interactions such as hydrogen bonds, Van der Waals, Coulombic or dipole interactions, π–π stacking or hydrophobic interactions[9,10,11]. The self-assembling units can be cross-linked polymers or low molecular weight gelators (LMWGs) and in this sense they are called molecular or supramolecular hydrogels (Scheme 1)[12].

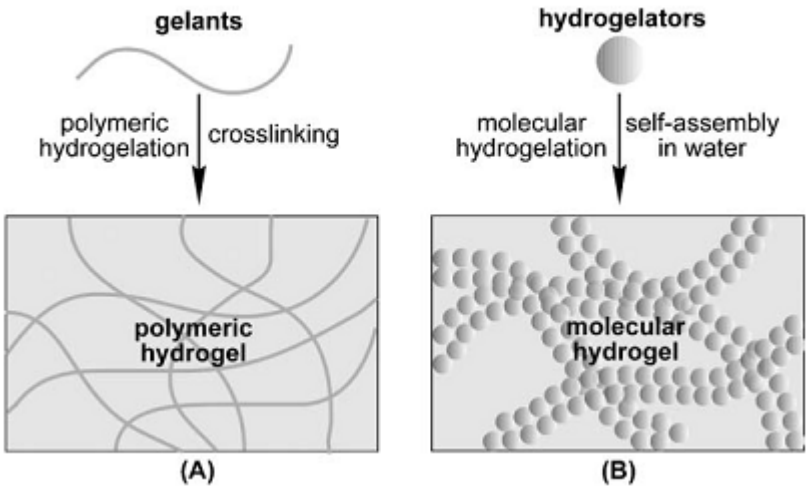

Scheme 1 Schematic diagram for (A) polymeric hydrogel and (B) molecular hydrogel.[12]

1.3. LMWGs and self-assembly process.

LMWGs include bioactive molecules such as amino acids or peptides, usually with molecular weight bellow 1000 Da. The literature[13-15] reports that this kind of system is more biocompatible than the ones manufactured by the polymeric approach, being incorporated in a wide variety of biomedical devices in many areas such as:

- Cell scaffolding for tissue engineering – as media for cell differentiation, molecular hydrogels offer the advantage of a 3D scaffold for *ex vivo* growth of cultured tissue cells[12]. This is an expressive advantage compared to the usual 2D growth procedures, which fail to reproduce the *in vivo* environment for cell differentiation. For example, it is common to find serious perturbations in gene activation and protein expression processes with 2D growth procedures[16]. Authors mention that the success in using biocompatible molecular noncovalent hydrogels results from the dynamic nature of the network of fibrils which allows the material to spontaneously adjust to the surrounding environment[12]. Each type of cell culture requires a different medium with specific mechanical properties[17], stimulating much research in the design and synthesis of structurally diverse LMWGs candidates.

- In the pharmaceutical technology field: the intrinsic network of hydrogels can protect drugs from environmental factors, like the presence of enzymes or different pH environments found in living organisms. Hydrogels can also control drug release through gel structural changes trigged by sol-gel phase transition processes[18].
- In regenerative medicinal processes: this approach is based on the ability of this kind of colloidal systems to assist cell adhesion, promote growth of neurons or to direct bone mineralization[19].

Molecular self-assembly can be described as the spontaneous formation of ordered structures under thermodynamic and kinetic control, through noncovalent interactions between molecules[20,21]. Hierarchical nanostructures or macroscale fragments arise from the self-association process.

Self-assembly is crucial for life maintenance processes, like the organization of phospholipids into biological membranes, DNA double helix assembly through hydrogen bond interactions, disposal of microtubules or microfilaments along the cellular life cycle phases. It also gives rise to the amyloid fibrils, which are proposed to be the cause of neurological diseases like Alzheimer´s[21].

Despite the high number of publications reporting the preparation of noncovalent self-assembled hydrogels, there is a lack of understanding on how media composition determines the properties of colloidal network structures and about the laws that govern the dynamics of molecular gelation phenomena. In other words, there is a need for the development of a relationship between the noncovalent forces that drive self-assembly processes and hydrogelation[22].

Amongst self-assembling LMWGs systems, **peptide-based molecular hydrogelators** attracted the most extensive research efforts, owing probably to its versatile synthetic pathways, excellent gelation ability, good biocompatibility and easy tuning of bioactivity[23-25].

When peptide molecules start to assemble, in response to pH changes or by cooling super-saturated media, three situations are possible (Figure 3): (A) crystallization, in response to highly ordered packing; (B) formation of amorphous precipitate or (C) an aggregation process yielding a gel. The process of gelation involves self-association of

molecules to form long, polymer-like fibrous aggregates, which get entangled during the aggregation process leading to a matrix that traps solvent, mainly by surface tension. This process prevents the flow of solvent under gravity and the material appears like a solid[26].

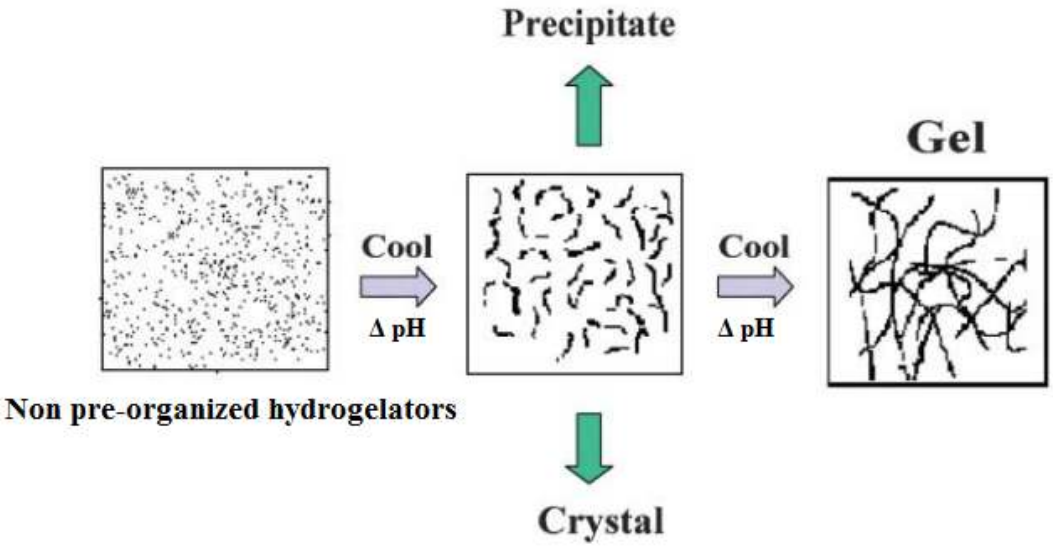

Figure 3 Schematic representation of different aggregation modes for peptide-based molecular hydrogelators.[26]

1.4. Design of LMWGs.

Observing the protein motifs pattern, researchers realized that peptide self-assembly is driven by intermolecular interactions, such as hydrogen bonding, ionic, electrostatic, hydrophobic and Van der Waals interactions. Knowledge from molecular and structural biology has inspired the design and synthesis of increasingly complex self-assembled biomaterials for biomedicine and bionanotechnology. By engineering the amino acid sequence, the secondary structure of peptides can be manipulated to optimize interactions between adjacent peptides. Long-range organization of peptide monomers produces nanofibrils which aggregate into 3D fibrous networks[27].

There are many strategies to design self-assembling molecular materials based on peptides and their derivatives. For peptides containing at least ten amino acids, the supra-molecular structures observed are more frequently coiled-coils (α helical based systems), β-sheets, β-hairpins, π-stacking systems and peptide amphiphiles [28a].

β-sheets consist of multiple peptide chains displaying an extended backbone arrangement that permits hydrogen bonding between the backbone amides and carbonyls. Each chain is referred to as a strand; the hydrogen bonded strands are referred to as a sheet. β-sheets can be orientated so that all their C-termini are at one end of the structure, described as a parallel structure, or so that the N and C termini alternate, described as an anti-parallel structure. β-sheets are well known for their ability to assemble into long fibrous structures. A number of different hierarchical structures can be formed from β-sheet peptides: tapes, ribbons, fibrils and fibres, all of which vary in the number of sheets that pack together to form the final structure[28a] (Fig 4). For a given peptide sequence, the formation of higher order structures is controlled by peptide and salt concentration. Increasing peptide concentration allows a higher assembly level.

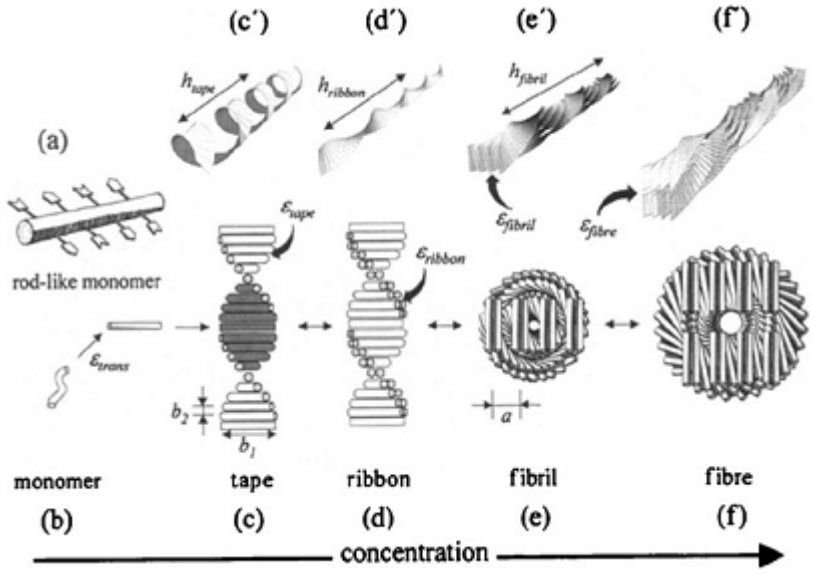

Figure 4 β-sheet based fibres can form a series of hierarchical structures depending on the concentration. These structures range from the basic peptide structure (a) as a monomer (b) which assembles into a tape (c and c′), two of which can bury hydrophobic residues by forming a ribbon (d and d′). Ribbons can further assemble by

lying face to face to form fibrils (e and e´) and additionally side by side to form fibres (f and f´). Adapted from Ref. 27a [28a].

β-hairpins consist of two short β-sheet sequences linked by a turn sequence (Fig. 5). This motif consists of two antiparallel β-strands, adjacent in the primary structure, linked by a short loop of two to five amino acids. β-hairpins can occur isolated or as part of a series of hydrogen bonded strands that collectively compose a β-sheet.

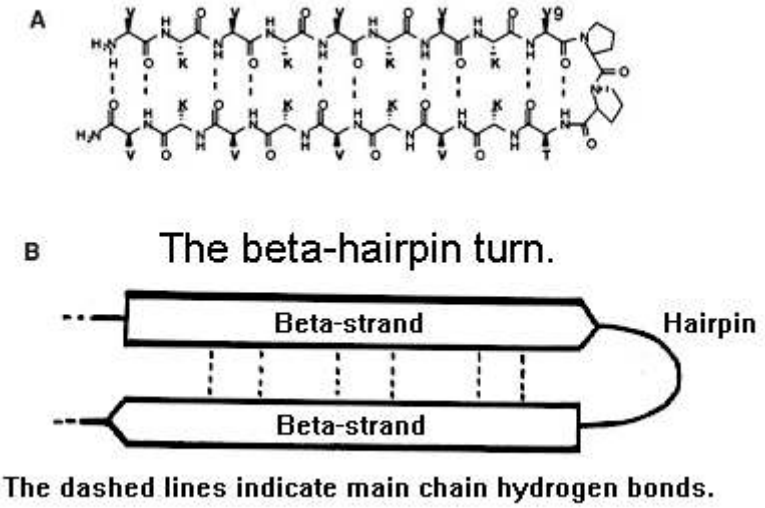

Figure 5 β-harpin structure: (A) peptidic sequence showing hydrogen bonds and a proline bridge which characterizes the β-harpine turn; (B) cartoon scheme of the β-harpin turn. Adapted from Reference 28a[28a].

For the purpose of self-assembly, α-helices are used as components of coiled-coils. The coiled-coil has characteristic amino-acid heptad repeats designated as *a to g* in one helix and *a´ to g´* in the other. The hydrophobic residues occupy positions at the interface of the two helices (*a, d* and *a´, d´*) whereas *e, g* and *e´, g´*, which are usually solvent exposed polar residues, give specificity between the two helices through electrostatic interactions (Fig. 6). Coiled-coils provide an opportunity to prepare peptide-based nanofibrous structures based on well established design rules derived from natural systems[28b].

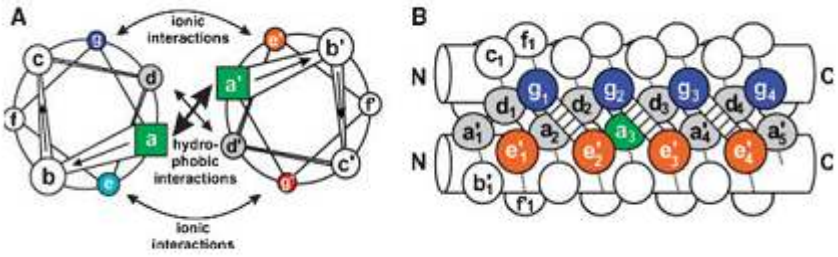

Figure 6 Schematic representation of a dimeric coiled-coil: (A) top view of the helical wheel representation, down the axis of the α-helices from N-terminus to C-terminus; (B) side view. The residues are labeled *a*-*g* in one helix and *a´*-*g´* in the other[28b].

Peptide amphiphiles are oligo-peptides modified with a hydrophobic alkyl tail to form molecules with distinctly hydrophobic and hydrophilic ends, similar to lipids. The basic overall chemical structure of a peptide amphiphile and its self-assembly into macrostructures is shown in Figure 7. The alkyl tails form the hydrophobic core of the nanostructures. A glycine based sequence is required for providing hydrogen bonding links in order to put the structure together, whereas the outer polar residues ERGDS (glutamic acid, arginine, glycine, aspartic acid and serine) in the peptide are free to adopt a random structure.

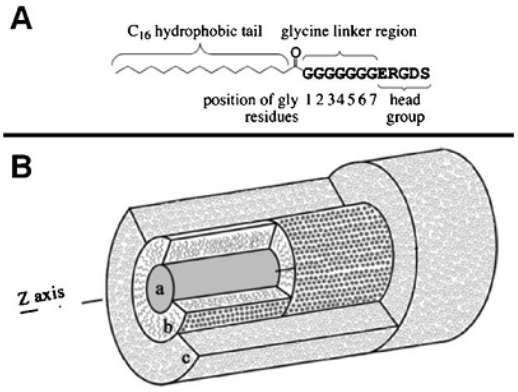

Figure 7 (A) Chemical structure of a peptide amphiphile. (B) Cartoon representation showing the supramolecular arrangement of the peptide amphiphiles: (a) the alkyl chains form the core; (b) glycine linker and (c) polar head groups[28a].

Taking into account the motifs present in naturally occurring proteins, scientists have moved towards designing new short self-assembling peptides amenable to functionalization[27]. As peptides are so versatile building blocks, small peptides or even single modified amino acids can self-assemble into networks, capable of entrapping water and form hydrogels. This bottom-up approach lays its foundation on the high level of self-assembly specificity of peptides, which is mainly dependent on the recognition of intermolecular interactions between side chains in the peptide sequence.

Fibers[29,30], tapes[31], tubes[32] and spheres[33] are the main types of nanostructures designed and built from low molecular weight hydrogelator species. One possible approach to prepare supramolecular hydrogels from LMWGs is the use of cyclic peptides designed with an even number of alternating of D- and L-amino acids, that interact with each other to form nanotube arrays as shown by Ghadiri *et al*[34a].When protonated, these compounds crystallize into tubular structures with hundreds of nanometers long and internal diameters of 7–8 Å (Figure 8).

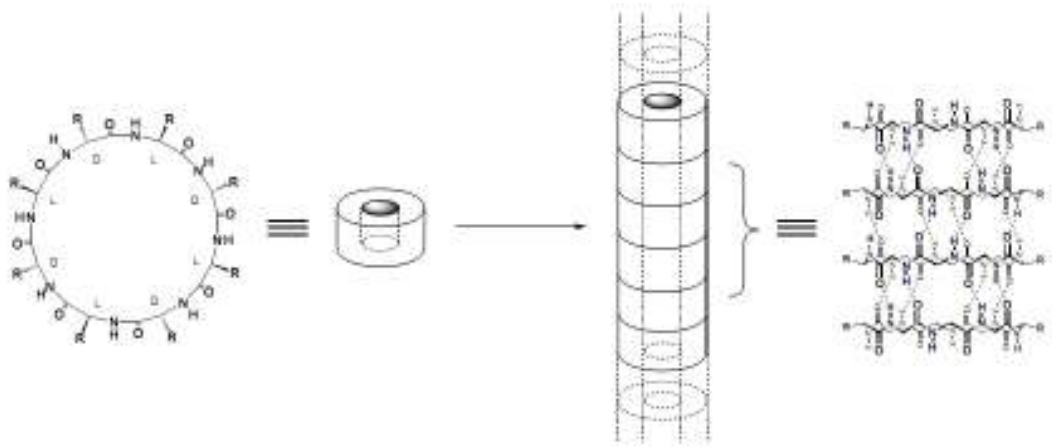

Figure 8 Schematic diagram of nanotube assembly from cyclic D,L-peptides[34b].

Amphiphilic peptides are also being used to prepare nano-assemblies as demonstrate by Hartgerink *et al*[35]. This author used self-complementary ionic peptides, which pack into a β-sheet conformation, to prepare self-assembled nano-fibers[35] (Figure 9).

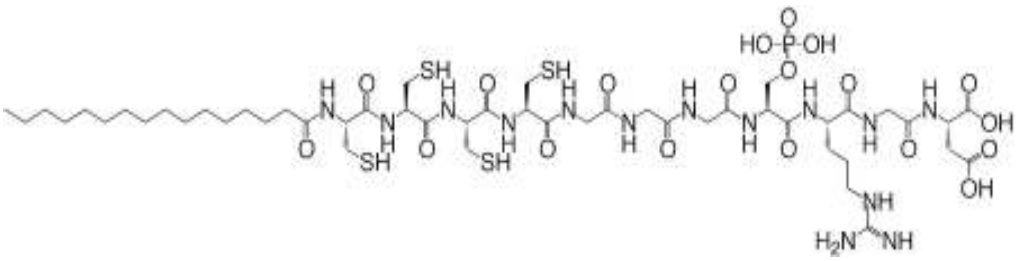

Figure 9 Chemical structure of one amphiphilic peptide synthesized by Hartgerink *et al*[35].

Zhang *et al*[36] investigated four G_nD_2 peptides, composed of a well-defined hydrophilic aspartic acid (D) sequence linked to a glycine (G) hydrophobic fragment (where n = 4, 6 or 8). They found that these surfactant-like peptides represent another example of hydrogelators that self-assemble into nanotubes and nanovesicles in water at neutral pH (Figure 10). The glycines are packed inside of the bilayer away from water and the aspartic acids are exposed to water, much like other surfactants.

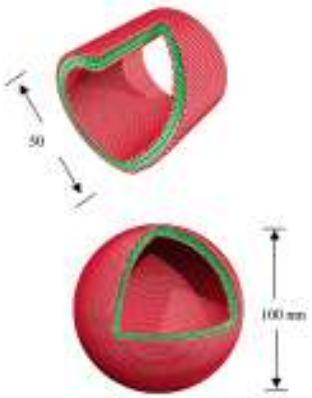

Figure 10 Molecular modeling of the structures formed from the peptides with negatively charged heads and glycine tail. (A)Peptide nanotube and B)Peptide nanovesicle. Color code: red, negatively charged aspartic acid heads; green, nonpolar glycine tail[36].

In addition, Yokoi *et al*. reported the assembly of the ionic self-complementary peptide RADA16-I (Figure 11) into a nanofiber scaffold composed of β-sheet structures that eventually becomes a hydrogel consisting of more than 99.5% of water[37].

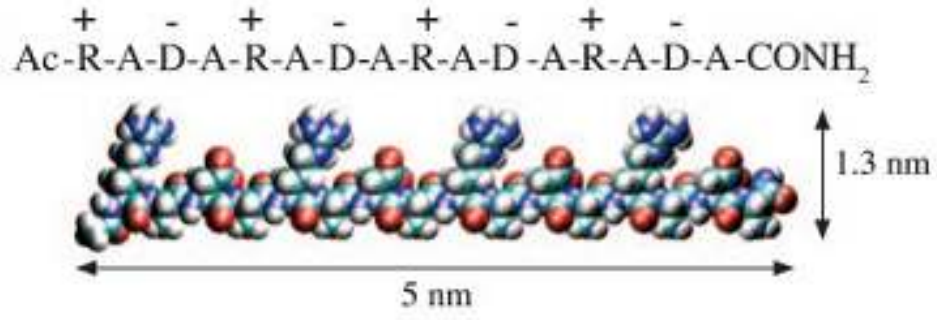

Figure 11 Peptide RADA16-I: amino acid sequence and molecular model of RADA16-I; Ac: acetyl moiety; A: alanine; D: aspartic acid and R: arginine[37].

Nowadays, there is a trend for basing the design of LMWGs in the ability of peptide molecules to pack each other via **aromatic-aromatic interactions**. There are many examples in literature showing that the hydrogel forming ability of short peptides (di or tripeptides) or even single amino acids, is significantly enhanced by **π-π stacking interactions**. Some works point out that this kind of aromatic interaction is likely to impart the ideal balance between hydrophilicity of polar groups, responsible for solubility, and hydrophobicity attributed to non-polar groups which is relevant to the self-assembly of peptides[38]. π-π Stacking interactions are found in amyloid peptides, which contain the phenylalanylphenylalanine motif. This dipeptide is able, on its own, to self-assemble into stable peptide nanotubes[39], believed to be the cause of Alzheimer´s disease.

Amongst reports exploring the π-stacking feature, there are important results related to the chemical coupling of a variety of aromatic groups to short peptides. Linking aromatic groups such as fluorenyl[24,40] (A), naphthyl[19,41] (B, C and D), benzyl[42,43] (E) or pyrenyl[44] (F) to the N-terminus endows some peptides, and even single amino acids, with the ability to form stable hydrogels[45](Fig. 12).

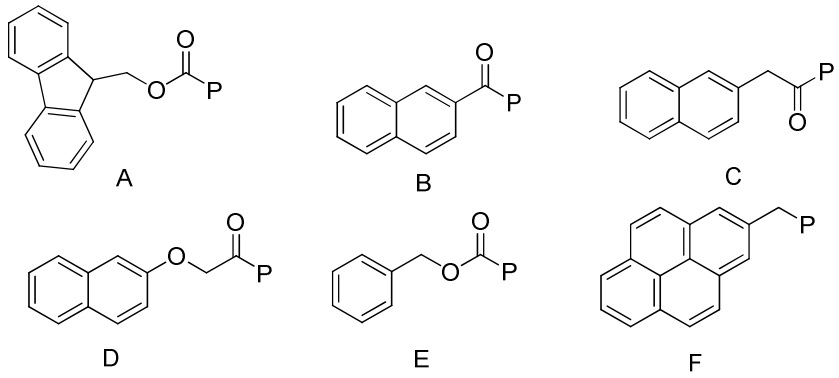

Figure 12 Examples of π-stacking inducing groups frequently employed in the synthesis of hydrogelators.

The hydrophobicity of the peptides is another relevant parameter determining gel formation capacity. Johnson *et al*. mention that dipeptides should display ideal hydrophobicity, expressed by the value of log P, to become potential hydrogelators[43]. These authors report that weak and unstable gels are formed by peptides with log P values below 2.8, whereas dipeptides with log P values above 5.5 appeared too hydrophobic to form homogeneous gels. At intermediate values of log P (3.4–5.5), all dipeptides assembled yielding gels of similar strengths[46].

In addition to π-stacking and molecular hydrophobicity, there are many works demonstrating the importance of the hydrogen bonding interaction for the self-assembly process of supramolecular hydrogels. Many considerations have arisen in the literature about the pKa control of the hydrogelation process[43,46]. Some works show that carboxilated peptides form gels depending on the extent of protonation of this functional group and that gelification occurs when the carboxylic acid is protonated[46,47]. One interesting observation is that dipeptides cross-linked in a hydrogel network, display pKa values superior to the free solvated peptides in aqueous media. The incorporation of the carboxylic acids into an highly hydrophobic environment is a reasonable explanation[48]. Another theory is that the increment in pKa results from stabilization of the carboxylic acid group by the neighboring dispersed dipeptides[43].

Another interesting observation is that seemingly minimal modifications, such as permutation of the C- and N-terminal amino acids in peptide sequences, can result in completely different materials as shown by Cheng *et al*[49]. These authors describe

that the hydrogel formed by tripeptide Fmoc-Lys-Leu-Val-OH is composed by a network of fibrils while the Fmoc-Val-Leu-Lys-OH hydrogel shows high level of alignment in its fibrils. An additional example is provided by Adams *et al*[50], who found that the dipeptide Nap–Ala–Gly–OH is able to form hydrogels by just tuning pH, whilst Nap–Gly–Ala–OH precipitates under the same conditions. Molecular modeling based on X-ray diffraction studies, suggests that the different behavior observed for peptides Nap–Ala–Gly–OH and Nap–Gly–Ala–OH could be ascribed to different conformations and hydrogen bond preferences.

The degradation kinetics of hydrogels´s matrix has to be taken into account in the design of hydrogelators. In this context, it is reasonable to assume that hydrogels formed by natural proteinogenic peptide sequences are prone to degradation by endogenous proteolitic enzymes. Introducing non proteinogenic amino acids into peptide sequences could be useful to increase the proteolitic stability of hydrogels. Peptides bearing non proteinogenic amino acids are being investigated in our research group and in other research groups as potential hydrogelators. Non proteinous β-amino acids, namely β-alanine residues, have recently been incorporated into dipeptide hydrogelators. This modification yielded enzyme resistant hydrogels, which were used as matrix for controlled-release of vitamins B_{12} and B_2 at physiologic conditions[51]. A supramolecular hydrogel based on (non natural) D-amino acids, resistant to proteinase K catalysed-hydrolysis and exhibiting, thus, long-term bio-stability and *in vivo* controlled drug release, was prepared by Xu *et al*.[52]

The introduction of non proteinogenic amino acids into peptides was also explored by Gupta *et al*[53] who evaluated the self-assembly process of a dipeptide made of phenylalanine and α,β-dehydrophenylalanine. This non-coded achiral amino acid is known to introduce constraints into molecular structures[54,55,56]. Non-proteinogenic peptides offer the advantage of being less susceptible to enzyme degradation. Moreover, non proteinogenic amino acids can add a positive contribution to the balance of the thermodynamic forces that modulate peptide aggregation and water swelling processes. More rigid structures should lead to a lower reduction in entropy when molecules self-assemble.

Hydrogels with intrinsic medicinal properties can be created by incorporating known therapeutic motifs, as organic modifiers, into hydrogelators. Anti-oxidants such

as catechol-derivatives have been introduced into chitosan/pluronic composite hydrogels. These materials revealed improved tissue adhesion, characteristic of this type of hydrogels, ideal for developing drug delivery systems, tissue engineering applications or even as tissue adhesives to arrest bleeding[57].

1.5. Methods for characterization of hydrogels

The usual methods for characterizing the molecular arrangement of nanofibrils in hydrogels are inherently low-resolution[9]. UV-vis absorption, Fourier Transform Infrared spectroscopy (FTIR), fluorescence and circular dichroism (CD) spectroscopy can be used to evaluate the characteristics of the secondary structure and electronic properties of these materials[58].

FTIR spectroscopy is employed to confirm the presence of H-bonds and determine the protonation state of carboxylic acids[59-62]. The C=O and N-H stretching vibration bands from terminal carboxyl and amide groups directly reflect their ionization state and potential involvement in hydrogen bonds[62,63]. Some bands of interest (like NH stretch) can appear overlapping the OH stretch of water. Thus, FTIR analysis of hydrogels is often performed using dehydrated samples. These outputs need to be analyzed with caution, since structural modifications may occur due to water loss.

UV/Vis characterization of hydrogels is usually conducted using two different approaches. One possibility is to incorporate spectroscopic fluorescent probes into gelators[64,65]. This is an effective design strategy; the large, flat aromatic surfaces of fluorophores are likely to promote aggregation and, at the same time, a powerful tool for evaluating the aggregation hydrophobic pockets[66]. UV/Vis is also used to detect changes of hydrophobicity in the surroundings of reporter groups. Both, intrinsic reporter groups, making part of the gelator molecule, or added extrinsic probes, can be used to identify π-π stacking or metal coordination trigged aggregation[58].

The secondary structure content of protein aggregates is an important parameter as specific secondary structures are characteristic of different stages in aggregation

pathways. For example, in β-amyloid peptide, associated with Alzheimer´s disease, monomers and small oligomers have been found to consist of mainly disordered/α-helical structures; intermediate fibrillar oligomers are annular protofibril and ending fibril conformers contain mostly β-sheet secondary structure.

A single, straightforward protocol is not currently available to estimate the content of each type of secondary structure in self-assembled peptide structures. Instead, researchers employ a host of scientifically acceptable approaches to estimate secondary structure content from raw Circular Dichroysm (CD) and FTIR data. CD is an analysis technique that measures differential absorption of right and left polarized light while FTIR analyzes molecular bond vibration frequencies[67-69]. Comparing general features of CD or FTIR spectra with controls or "expected" results, often allows to infer secondary structure changes or to quantify overall secondary structure content of proteins[70a]. Illustrative examples of CD spectra characteristic of β-sheet, α-helix, and unordered/random coil secondary structures are shown in Figure 13 for the polypeptide poly-L-lysine and for the placental collagen protein[70b].

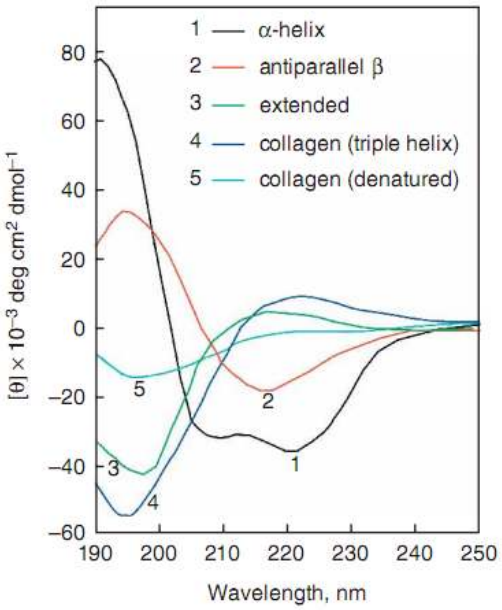

Figure 13 CD spectra of poly-L-lysine: (1) α-helical conformation (black), (2) anti-parallel β-sheet conformation at pH 11.1 (red), (3) extended conformation at pH 5.7 (green) and placental collagen: (4) native triple-helical (blue) and (5) denatured forms (cyan). Note that the extended conformation of poly-L-lysine was described as a random coil[70b].

In a typical CD spectrum of a protein, there is a weak, but broad, n-π* transition centered around 210 nm and an intense π-π* transition about 190 nm. Studies of far UV CD can be used to assess quantitatively the overall secondary structure content of the protein, since it has been known for many years that the different forms of regular secondary structure found in peptides and proteins exhibit distinct spectra[70c].

The near UV CD of proteins arises from the environments of each aromatic amino acid side chain as well as possible contributions from disulphide bonds or non-protein cofactors which might absorb in this spectral region. Small model compounds of the aromatic amino acids exhibit CD spectra because the chromophore is linked to the nearby chiral α-carbon atom. In the case of proteins in their native states, the side chains of these amino acids will be placed in a variety of asymmetric environments characteristic of the tertiary structure of the folded protein. A number of factors can influence the CD spectra of aromatic amino acids. Among these are: the rigidity of the protein, with the more highly mobile side chains having lower intensities; the nature of the environment in terms of hydrogen bonding, polar groups and polarizability. In addition the CD spectrum can be altered by interactions between aromatic amino acids which are especially significant if the distance between them is less than 1 nm. In the "exciton coupling" model, two excited states of chromophores, in close proximity, result from exciton mixing of the two strong transitions; the states correspond to symmetric and antisymmetric combinations of the excited state wave functions. The two resulting CD bands will overlap with some cancellation (the extent of which depends on the size of the interaction), giving rise to a sigmoidal CD curve. A final factor is the number of aromatic amino acids in a protein. Proteins with large numbers of such amino acids can have smaller CD bands than might be expected because of cancelling effects of positive and negative contributions[70c].

TEM, cryo-TEM and SEM are electron microscopy techniques useful to elucidate fibril dimension and morphology, parameters relevant to infer length-to-mass information about fibril building blocks[22]. Diffraction methods, including small-and wide-angle X-ray, neutron and electron diffraction are appropriate to reveal the molecular packing distances in the nanostructures and its dimensions *in situ*[9].

However, to establish a better relationship between monomer structure, assembled nanostructures and emergent hydrogel properties, it´s imperative to apply high-resolution structural characterization methodologies[9].

Crystallographic techniques are suitable for characterizing the atomic structure of molecules. However, in order to be analyzed by these methods, the peptide hydrogelators have to be crystalline materials, which often is not the case, as observed for the amyloid peptides. That's why sometimes is hard to implement this method for the characterization of peptide self-assembled materials[22,71]. Moreover, it is necessary to take into consideration that the scattering pattern obtained from single crystals differs from that obtained from the nanofibers that compose hydrogels. Despite these observations, it is accepted that single crystals provide good approximations of the hydrogel state and that crystallographic methods are a powerful tool to allow further insight into the architecture of self-assembled hydrogels at the molecular level[72,73].

Solution phase NMR is ineffective for investigating self-assembled materials as hydrogelator assembly into higher order structures broadens NMR signals due to anisotropy effects[74,75]. On the other hand, the successful application of solid state (SS-NMR) to the analysis of amyloid fibrils[76], gives rise to the possibility of using this methodology to analyze hydrogels on its native gel state. Isotopic labeling bidimensional SS-NMR methods have been shown effective for mapping β-strand motifs in several amyloid-forming proteins[77-79]. This opens the possibility of characterizing cross-β fibril structures, which have many similarities to the nanofibers observed in hydrogels´s network.

The information acquired through both low and high resolution techniques, can give more robust insight into the parameters that govern the self-assembling process. These techniques can provide constraints crucial for the development of computational models that can describe hydrogels systems and help to design new hydrogelators displaying desirable rheological properties or targeted behavior features. This kind of approach has been implemented to develop theoretical models to the amyloid systems, and seems satisfactory[9].

This work reports the synthesis and characterization of new modified peptides that contain phenylalanine and a dehydroamino acid and investigates their potential as hydrogelator agents. The temperature and pH dependence of the gelification process

were also evaluated. The organic modifiers were chosen aiming to increase the aromatic character of the peptides, which could lead to more efficient hydrogelators suitable as biomaterials.

For this purpose, multi substituted (bi and tri substituted) benzene derivatives were designed by attaching the above mentioned dehydrodipeptides (DHD) to the modifiers trough amide linkages. The new molecules have C_2 (Fig. 14) or C_3 (Fig. 15) symmetry. These molecular architectures can be interesting for generating different patterns of cross-linked networks, which could influence the water trapping process. Moreover, the presence of multiple carboxylic domains can also make the hydrogels highly responsive to pH changes.

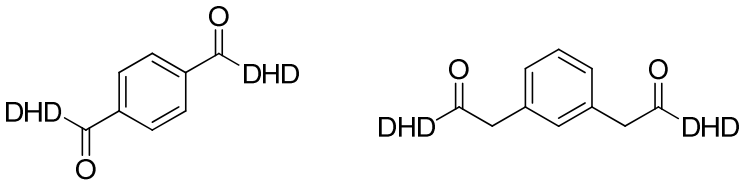

Figure 14 Class of C_2-symmetric compounds synthesized in this work as potential hydrogelators.

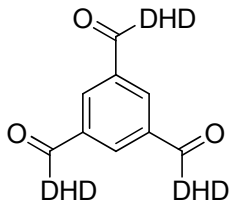

Figure 15 Class of C_3-symmetric compounds synthesized in this work as potential hydrogelators.

Recently, our research group discovered that conjugating dehydrodipeptides of these type with naphtyl motifs results in highly efficient hydrogelators with a monosubstitued pattern. In this sense, this work also includes the synthesis of monosubstitued molecules, where dehydrodipeptides are attached to the aromatic diphenylacetyl moiety

(Fig. 16). Our aim was to evaluate the effect of this different modifier on the gelation efficacy.

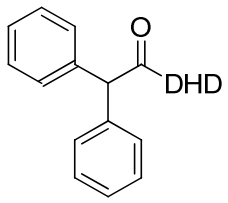

Figure 16 DHD monosustitued derivatives containing diphenylacetyl N-capping organic modifiers, synthesized in this work as potential hydrogelators.

Another class of monosubstituted derivatives was designed using catechol-derivatives, caffeic acid (CA) and dihydrocaffeic acid (DHCA), as aromatic modifiers (Figure 17). The catechol moieties could impart therapeutic properties to hydrogels, as these anti-oxidant compounds are known to display anti-inflammatory, antimutagenic, and anticarcinogenic activities[80]. Another potential advantage is that chatecol motifs are known to enhance tissue adhesion, making the hydrogels suitable for incorporation into many biomaterials[57].

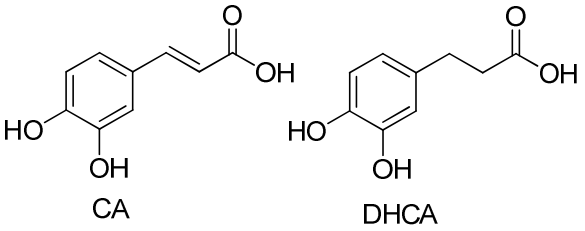

Figure 17 Chemical structure of dihydrocaffeic acid (DHCA) and caffeic acid (CA) molecules used as organic modifiers in this work.

The supra-molecular architecture of the prepared gels was studied using Scanning Transmission Electron Microscopy (STEM) and circular dichroism.

2. Objectives

Taking into account the experience of our research group in peptide chemistry, and especially in the synthesis of dehydroamino acids and dehydropeptides, we designed seven new modified dehydropeptides based on the attachment of different aromatic groups to dehydrodipeptides, through amide linkage.

The dipeptides synthesized in this work are composed of phenylalanine (Phe) linked to a dehydrophenylalanine (ΔPhe) or dehydroaminobutyric acid (ΔAbu) unit. Trimesoyl, terephtaloyl, 2,2´-(1,3-phenylene)diacetyl and diphenylacetyl derivatives were chosen as aromatic modifiers (Scheme 2). These modifiers were chosen aiming to take advantage of the thermodynamically favorable aromatic-aromatic interaction in water, which plays an important role in protein stabilization and probably is also important to direct the self-assembly of small molecules in water.

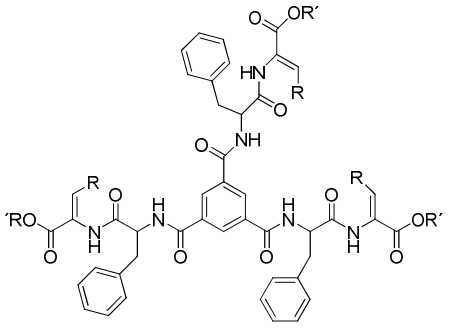

R=CH_3 e R´=CH_3, **13a;**
R=C_6H_5 e R´=CH_3,**13b**;
R=CH_3 e R´=H, **17a**;
R=C_6H_5 e R´=H,**17b**.

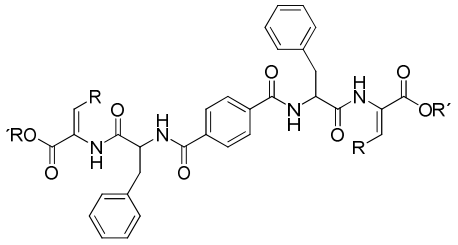

R=CH_3 e R´=CH_3, **14a**;
R=C_6H_5 e R´=CH_3,**14b**;
R=CH_3 e R´=H, **18a**;
R=C_6H_5 e R´=H,**18b**.

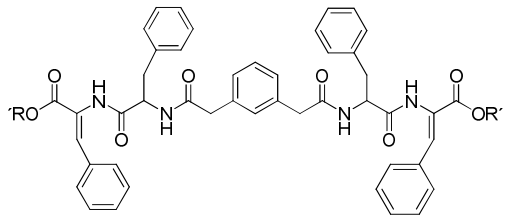

R´=CH_3, **15**;
R´=H,**19**.

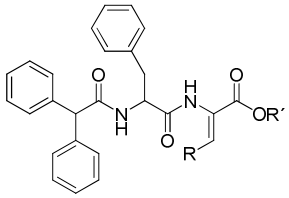

R=CH_3 e R´=CH_3, **16a**;
R=C_6H_5 e R´=CH_3,**16b**;
R=CH_3 e R´=H, **20a**;
R=C_6H_5 e R´=H, **20b**.

Scheme 2 Chemical structures of the synthesized dehydrodipeptide derivatives.

In addition, we have designed two other hydrogelators (Scheme 3) composed of the above mentioned dehydrodipeptide Phe-ΔPhe, N-capped with caffeic and dihydrocaffeic acid. The catechol-derivatives were chosen owing to their known medicinal properties and their potential of improving tissue adhesion.

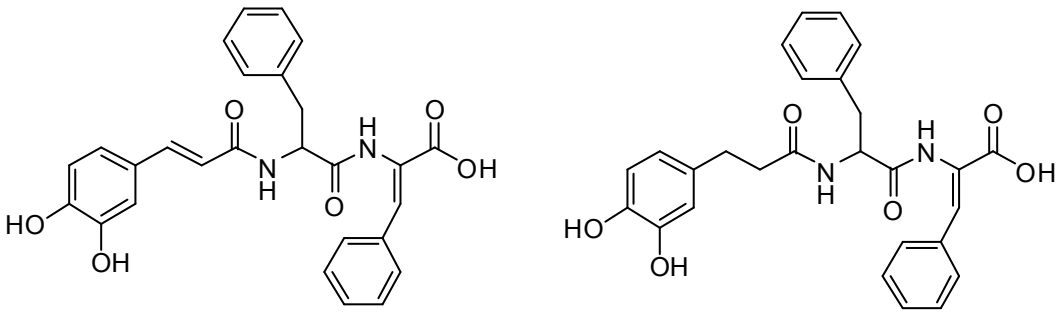

25 **27**

Scheme 3 Caffeic acid (**25**) and dihydrocaffeic acid (**27**) peptide derivatives designed in this work as potential hydrogelators.

We envisaged that the incorporation of the selected aromatic structures into dehydropeptides could enhance the propensity of the molecules to pack and form cohesive efficient hydrogel networks. Furthermore, we anticipated that hydrogels bearing more than one free carboxylic acid functional group could show an improved behavior towards water swallowing.

The non proteinogenic residues may make these structures more resistant to enzymatic hydrolysis. They could be also responsible for introducing conformational constraints into these new structures, leading to improved mechanical and chemical properties.

Finally, we expect that the information gained in the synthesis and characterization of the new materials will contribute to expand the understanding of the driving forces for self-assembly of peptide hydrogelators.

3. Results and Discussion

3.1. Synthesis of the modified α,β-insaturated peptides

The synthetic strategy employed in this work is based on coupling dehydrodipeptides to aromatic acyl chloride moieties, followed by ester hydrolysis under alkaline conditions, which resulted in the final dehydropeptides derivatives (Scheme 4).

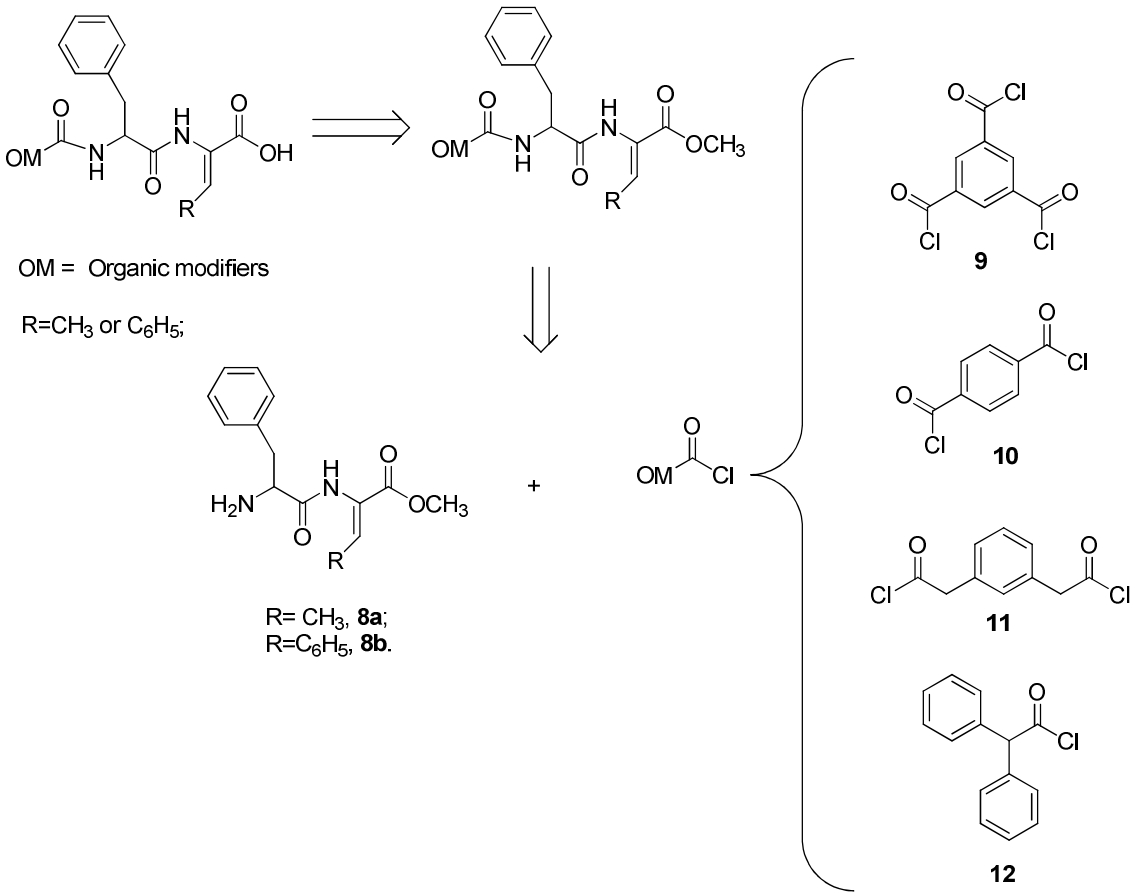

Scheme 4 Overview of the synthetic methodology employed for the synthesis of potential dehydropeptide hydrogelators.

3.2. Synthesis of the dehydropeptides

The production of the α,β-dehydroamino acids was the key step in the synthetic route. Amongst all the methods described in literature for the synthesis of α,β-dehydroamino acids, the most widespread is the dehydration of β-hydroxyamino acids, like serine or threonine, which yield the corresponding ΔAla and ΔAbu residues[81-83]. Other methodologies include the Hoffman degradation of α,β-diaminopropionyl residues[84], hydrolysis of unsaturated oxazolinones, reduction of azidoacrylates[85] or condensation of α-ketoacids with amines or nitriles[86,87]. However, most of these are low-yielding, multistep and non stereospecific methods, requiring a lot of effort to remove side products.

In this work, we have used methodologies developed in our research group for the synthesis of the α,β-dehydroamino acid synthetic blocks[88]. These consisted of 4-dimethylaminopyridine (DMAP) catalyzed reaction of β-hydroxyamino acids with *tert*-butyl pyrocarbonate [Boc_2O], followed by treatment with N,N,N',N'-tetramethylguanidine (TMG), which is known to lead to dehydroamino acids in high yields. The retrosynthetic pathway for the synthesis of dehydropeptides **8a** and **8b** is presented in Scheme 5.

L-phenylalanine (**1**) was protected with the *tert*-butoxycarbonyl group (Boc) using Boc_2O in a water/dioxane mixture. The methyl esters of DL-threonine (**2a)** and DL-3-phenylserine (**2b)** were prepared in high yields from the corresponding amino acids.

Coupling, using the dicyclohexylcarbodiimide (DCC) and hydroxybenzotriazol (HOBT) standard procedure, between *tert*-butoxycarbonylphenylalanine (Boc-L-Phe–OH- **4**) and methyl **3a** and **3b** afforded the corresponding dipeptides Boc-L-Phe-Thr(β-OH)-OMe **(5a)** and Boc-Phe-Phe(β-OH)-OMe **(5b)** with 52% and 78% yield, respectively. The byproduct dicyclohexylurea (DCU) precipitates from the reaction mixture as the reaction progresses.

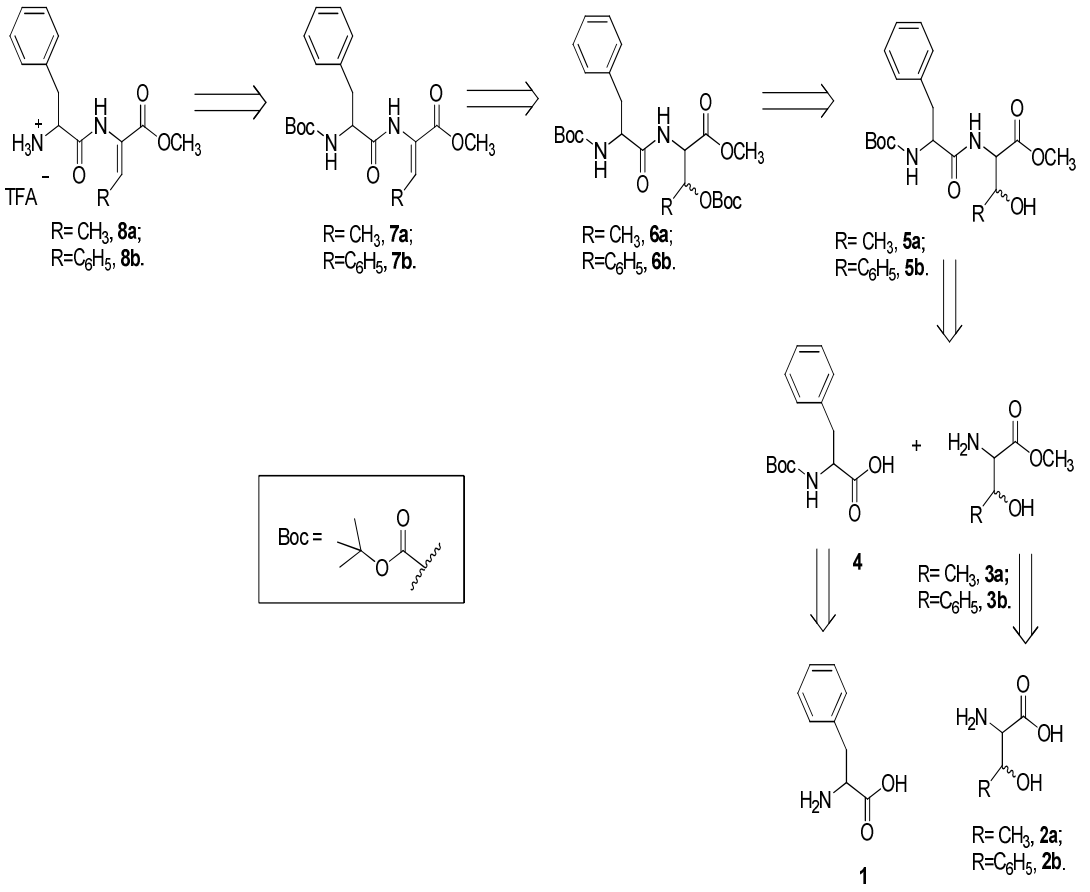

Scheme 5 Retrosynthetic analysis for the synthesis of the dehydrodipeptides Boc-L-Phe-Z-ΔAbu-OMe (**8a**) and Boc-L-Phe-Z-ΔPhe-OMe (**8b**).

Carbodiimide activation of amino acid derivatives often results in partial racemization of the amino acid. This happens because the intermediate O-acyl ureas are highly reactive and can lead to oxazolone intermediates, which rearrange giving undesired racemized products (Scheme 6).

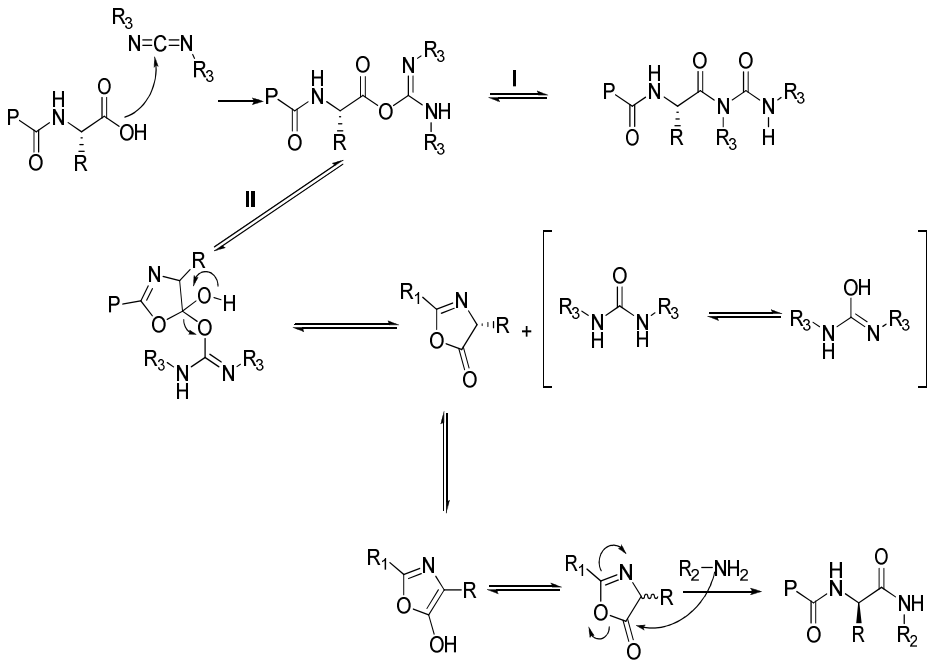

Scheme 6 Activation of the carboxylic acid group with a carbodiimide reagent and possible side reactions. I: rearrangement of the N-acyl urea derivative; II: racemization (P = protecting group, R = lateral chain of the amino acid, R_2 = carbon chain of the coupling amino acid; R_3 = alkyl chain of the carbodiimide compound).

To avoid this problem is useful to add to the reaction mixture one molar equivalent of 1-hydroxybenzotriazole (HOBt). The active hydroxybenzotriazole esters, formed as intermediates, couple to primary amines with little racemization. The mechanism is shown in Scheme 7.

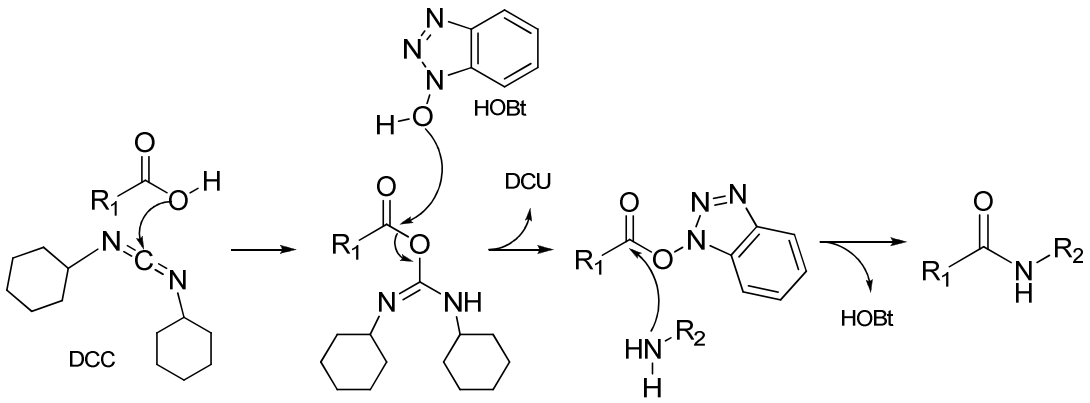

Scheme 7 Mechanism for the DCC/HOBt coupling reaction.

Dipeptides **5a** and **5b** were dehydrated by treatment with 1.1 molar equivalent of Boc_2O in the presence of a catalytic amount of DMAP. Without being isolated, the resulting O-tert-butylcarbonyl peptides **6a** and **6b** were reacted with TMG affording dedydrodipeptides **7a** and **7b** in good yields. DMAP catalyzes the acylation process promoted by the di-*tert*-butyldicarbonate reactant to yield O-tert-butyl carbonates which finally were dehydrated (in a one pot reaction) by the use of TMG. This reaction step appears to be stereospecific towards the more thermodynamically stable Z-isomer.

The stereochemistry of the α,β-dehydroamino acids was elucidated by NOE difference experiments, irradiating the α-NH protons and observing a NOE effect on the β-methyl or β-phenyl protons.

The Boc group was removed by treatment with trifluoracetic acid (TFA) (which protonates the nitrogen in the amide functional group, resulting in release of CO_2 and formation of t-butanol side-product) giving the desired products **8a** and **8b** as trifluoracetate salts with 87% and 92% yield, respectively.

3.3. Peptide coupling to aromatic modifiers

The N-deprotected dehydrodipeptides **8a** and **8b** were coupled to trymesoyl chloride **(9)**, tereftaloyl chloride **(10)**, 2,2´-(1,3-phenylene)diacetyl chloride **(11)** and diphenylacetyl chloride **(12)** to yield methyl esters **13a, 13b, 14a, 14b, 15, 16a** and **16b** (Scheme 8).

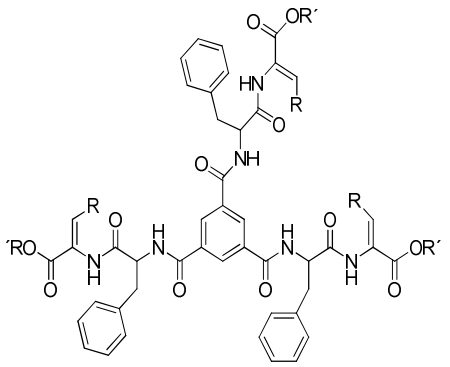

R=CH_3 e R´=CH_3, **13a**, 52%;
R=C_6H_5 e R´=CH_3,**13b**, 46%;
R=CH_3 e R´=H, **17a**, 82%;
R=C_6H_5 e R´=H,**17b**, 85%.

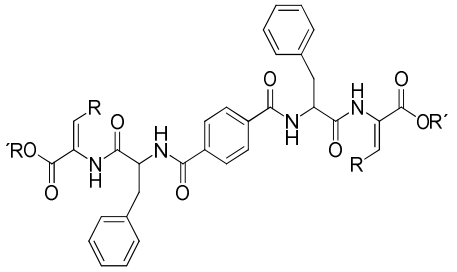

R=CH_3 e R´=CH_3, **14a**, 67%;
R=C_6H_5 e R´=CH_3,**14b**, 59%;
R=CH_3 e R´=H, **18a**, 68%;
R=C_6H_5 e R´=H,**18b**, 78%.

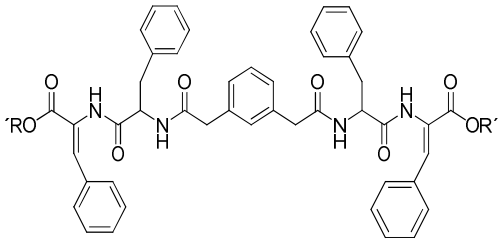

R´=CH_3, **15**, 47%;
R´=H,**19**, 64%.

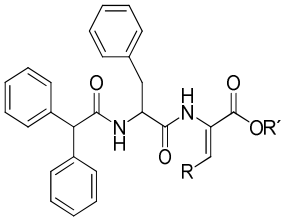

R=CH_3 e R´=CH_3, **16a**, 82%;
R=C_6H_5 e R´=CH_3,**16b**, 71%;
R=CH_3 e R´=H, **20a**, 71%;
R=C_6H_5 e R´=H, **20b**, 73%.

Scheme 8 Structure of the compounds obtained from the coupling reaction of **8a** and **8b** with organic modifiers. Isolated yields (%) are also indicated.

It was anticipated that the synthesis of multi-substituted hydrogelators based on the organic modifiers trimesoyl (**9**) and terephtaloyl (**10**) could reveal more challenging than the synthesis of simpler mono-substituted hydrogelators owing to steric crowding and unfavorable entropy contribution to the process.

In order to optimize the reaction yield, four different solvents were tested in the coupling reactions between peptides and the multi-substituted organic modifiers **9** and **10**. The best choice for both dehydrodipeptides was dry THF which afforded the highest yields (Table 1).

Table 1 Study of the effect of solvents on the isolated yield of the coupling reaction between organic modifiers **9** and **10** and dehydrodipeptides **8a** and **8b.** The dielectric constants (ε) and dipole moments (μ) of the applied solvents are also exposed.

Solvent	μ	ε	Yield* %			
			13a	**13b**	**14a**	**14b**
Toluene	0.36	2.4	12	13	15	11
CH_2Cl_2	1.6	9.08	22	18	33	27
THF	1.75	7.6	52	46	67	59
Acetonitrile	3.92	38	30	23	43	37

Dielectric constants and dipole moments in debye units from the compilation of solvent properties in J. A. Riddick and W. B. Bunger, eds., Organic Solvents, Vol. II of Techniques of Organic Chemistry, 3rd Edition, Wiley-Interscience, New York, 1970.

*isolated yields.

For the reactions studied, solvents that display high dipole moment and high dielectric constant afforded the best yields, indicating that the tetrahedral charged quaternary intermediate is probably better stabilized during the reaction pathway. The highest solubility of the TFA salts in polar solvents is another factor that can validate these data. However, acetonitrile which has the highest values of the above mentioned physical properties is not the best choice. This may be because the triethylamine hydrochloride by-product is more soluble in this solvent. In THF this by-product precipitates and this may push the equilibrium into product direction.

Refluxing at 80 °C for several hours was necessary to accomplish full substitution of the "multivalent" organic modifiers, whilst monosubstitued products **16a** and **16b** were synthesized at room temperature in higher yield. This probably reflects unfavorable entropy contributions to this type of reaction: there are more reactants species than products.

Compound **11** was generated in situ from the corresponding carboxylic acid and used without any purification. In this step, the carboxylic acid was reacted with $SOCl_2$ in the presence of DMF as catalyst to afford the Vilsmeier-Haack intermediate which reacts with the carboxylic acid to give the acyl chloride (Figure 18).

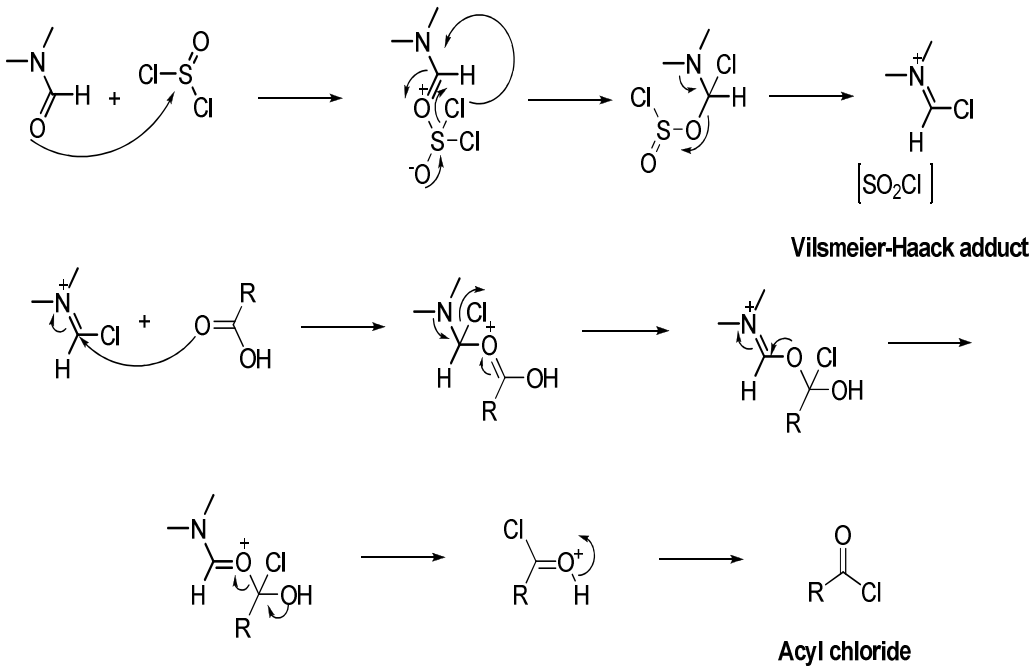

Figure 18 Mechanism for the DMF-catalyzed conversion of the carboxylic acid functional group into an acyl chloride via the Vilsmeier-Haack intermediate.

Compound **15** was also generated by another route (Scheme 9): the carboxylic acid group of 2,2'-(1,3-phenylene)diacetic acid **(21)** was activated by DCC/NHS (N-hydroxysuccinimide) and the active ester intermediate was reacted with (L)-Phe-OH **(4)**. In the second step, compound **22** was coupled to (DL)-Phe-(β-OH)-OMe **(3b)** via DCC/HOBt standard procedure. In the third step, compound **23** was dehydrated using the same procedure as described before.

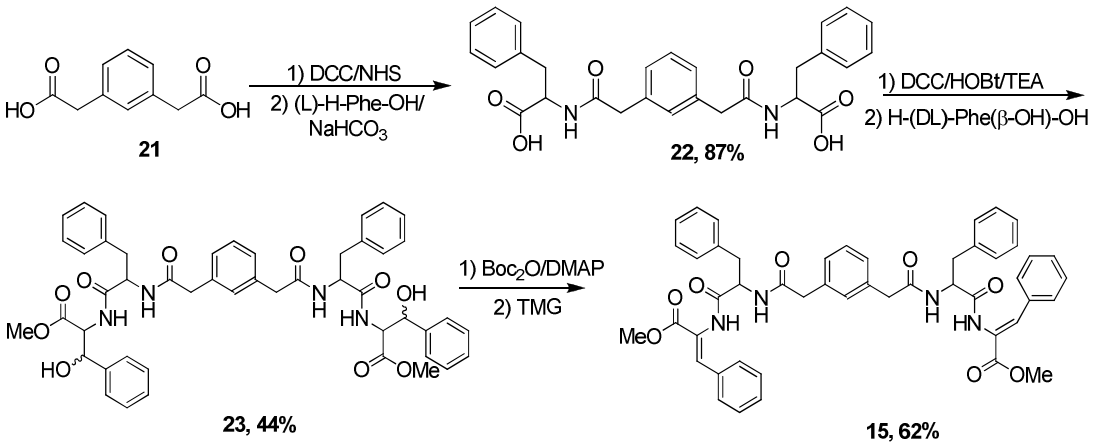

Scheme 9 Synthetic route to compound **15**: compound **21** was first reacted with L-H-Phe-OH (**4**) in basic media, than the isolated product **22** was coupled with (DL)-Phe-(β-OH)-OMe (**3b**). The product **23** was dehydrated affording **15**.

The DCC/NHS carboxylic activation process occurs according to the Scheme 10, where initially a reactive O-isoacyl urea (**III**) is formed which reacts with NHS (**IV**) to give a moderately stable ester (**V**) that react with the amine (**VI**) affording the correspondent amide (**VII**).

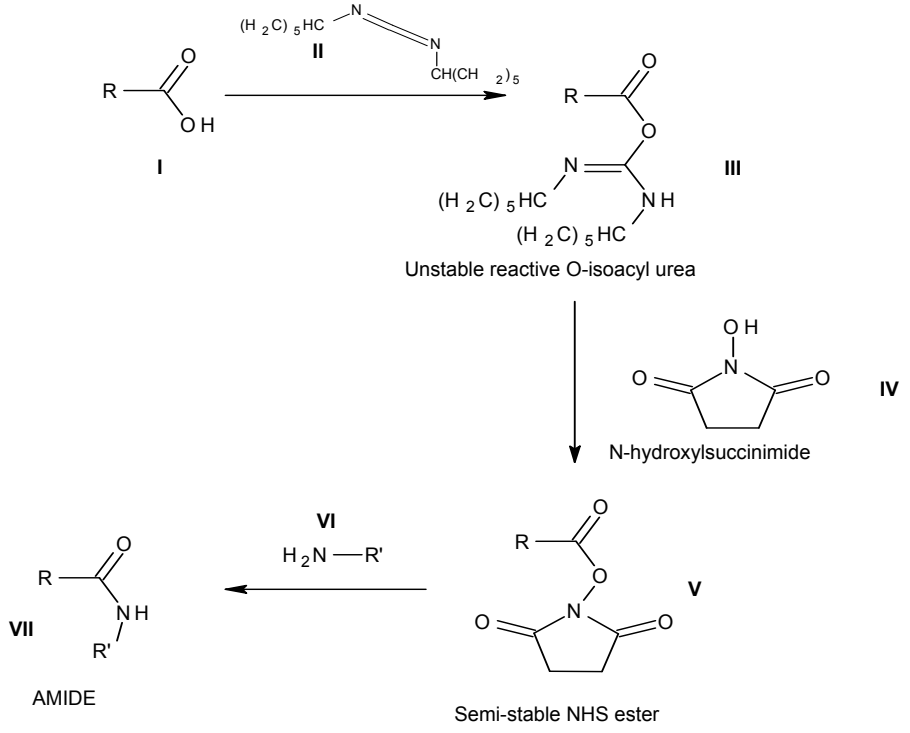

Scheme 10 Mechanism of DCC/NHS coupling.

The ^{1}H-NMR spectrum showed clear evidence of amide linkage formation without any evidence of isomerization of the target compounds. In Figure 19 is presented the spectra of compound **13b**. Characteristic signals and features, common to all dehydrodipeptide conjugates, are briefly discussed:

- The β protons (yellow) of phenylalanine appears as double doublets (dd) in the range of 3.0-3.3 ppm. These protons are classified as diasterotopic protons due to the presence of the chiral center at the α-carbon. There is a strong coupling between these geminal hydrogens and they couple with the α-proton with significantly different coupling constants. The α-proton and the β-protons have to be evaluated as an ABX system and the spectrum needs to be seen as a second order one. A and B represent the CH_2 β-protons which have similar chemical shifts and X corresponds to the α-proton that displays a significantly different chemical shift. The one that is less shielded couples with a higher coupling constant with the α-proton and its dd have a more complicated pattern because the relation $\Delta\nu_{\beta H-\alpha H}/J_{\beta H-\alpha H}$ is lower than the one for the other germinal proton;
- The ester protons (green) appear around 3.6-3.7 ppm as a singlet;
- The α-proton (orange) appears as multiplet in the range of 4.7-5.0 ppm and results from the couplings with the diasterotopic protons of the β-CH_2 and with the α-NH
- The aromatic protons appear in the region of 7.0-8.4 ppm;
- The amide proton (blue), that results from the coupling, has its signal around 8.6-9.0 ppm and is a doublet, because it couples with the α-proton;
- The amide ΔPhe α-NH proton (red) or the ΔAbu α-NH one appears as a singlet between 9.5 and 10.0 ppm.

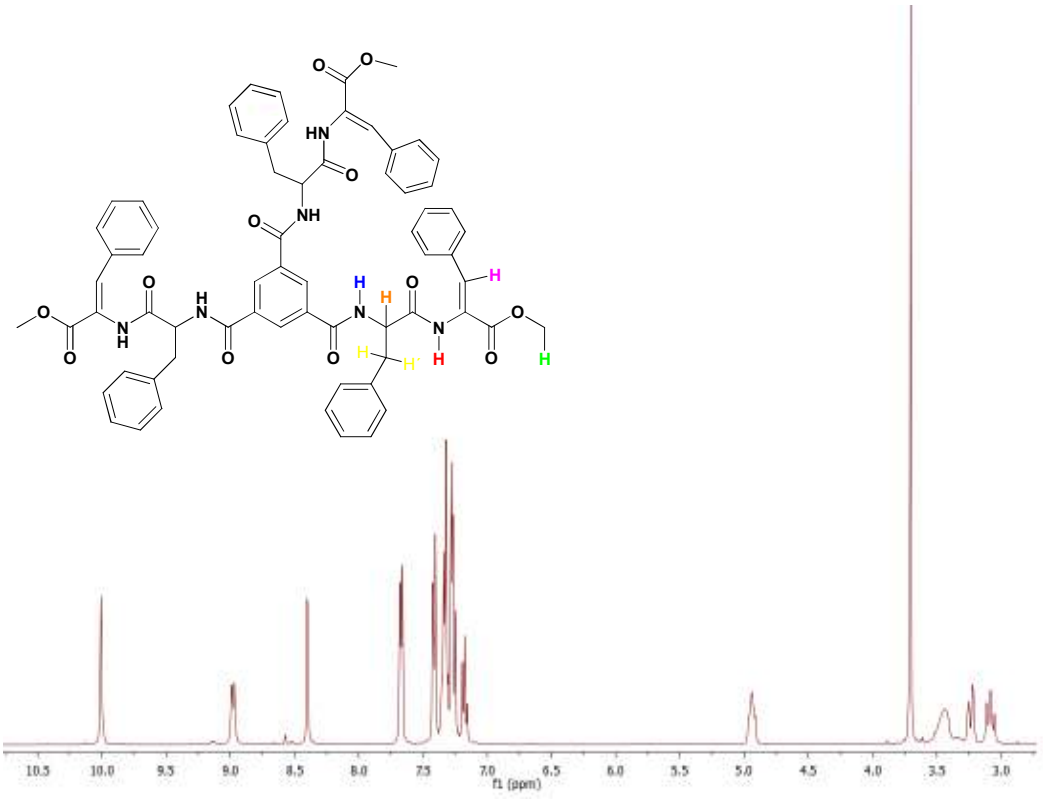

Figure 19 ^{1}H-NMR (400MHz) spectrum of compound **13b** in DMSO.

One peculiarity of dehydropeptide derivatives composed of phenylalanine and dehydropenylalanine is that the signal of the β-CH of ΔPhe (pink) appears in the aromatic region as a broad singlet.

The dehydropeptide derivatives containing the dehydroaminobutyric amino acid display the same pattern in the ^{1}H-NMR spectra as described above, with the difference that the β-CH of ΔAbu gives a quartet around 6.5-6.7 ppm and the γ-CH_3 protons appear in the region between 1.5 and 1.7 ppm as a doublet. These protons can be considered an A_3X system (two magnetic and chemically different groups of protons) originating a first order like spectrum with a coupling constant around 7.2 Hz in all compounds.

The final step in the synthesis involves ester hydrolysis under alkaline conditions in dioxane. The carboxylic acid derivatives were tested for hydrogel formation, as potential hydrogelators. In Figure 20 is shown the ^{1}H-NMR spectrum for hydrogelator **20a**.

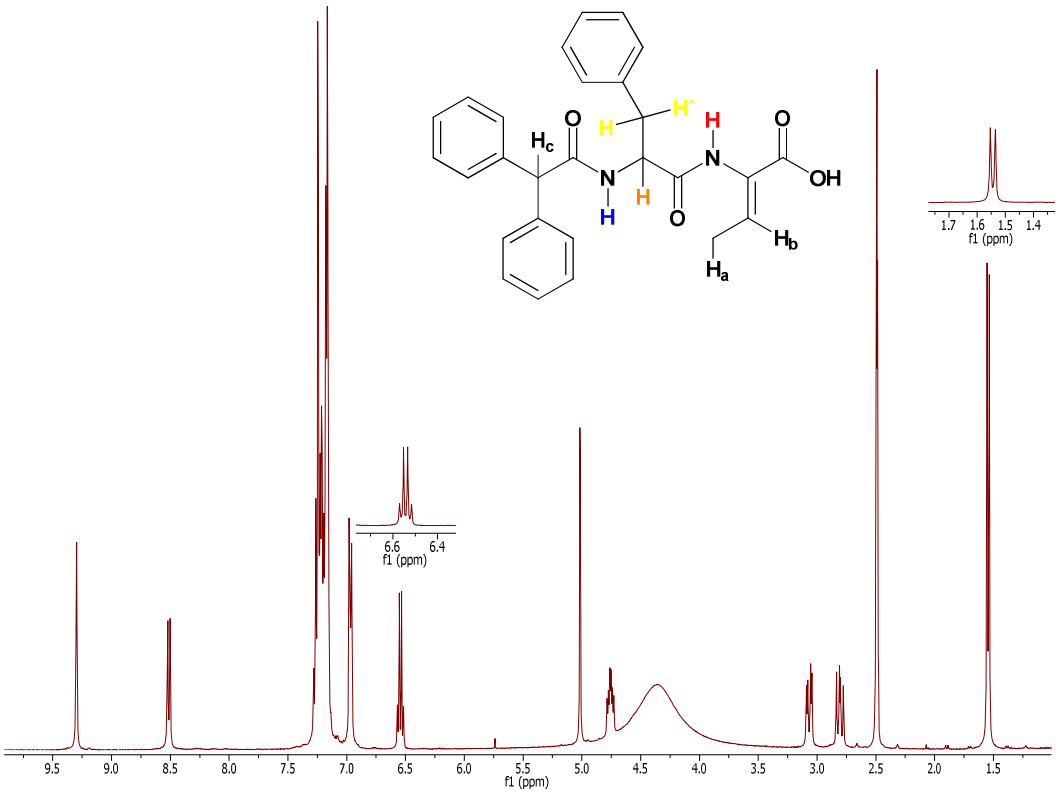

Figure 20 ^{1}H NMR (400 MHz) spectrum of compound **20a** in DMSO.

The signal assigned to the methyl ester protons in its precursor compound **16a** disappeared confirming the success of the hydrolysis reaction. In Fig. 20 are evidenced again the peculiar features described before for compounds that carry the ΔAbu motif. Apart the characteristic signals, the NMR spectrum shows a singlet around 5.0 ppm that is assigned to proton H_c, which appears also for compounds **16a**, **16b** and **20b.**

The ^{1}H-NMR spectra of compounds **15** and **19** display the same pattern discussed above, except for the fact that they contain signals assigned to the geminal CH_2 protons linking the central ring to the amide carbonyl, relative to the coupling to the dehydrodipeptide. These protons appear as two sets of doublets in the range of 3.2-3.4 ppm with coupling constants of 13.8 Hz. These characteristic features can be seen in the ^{1}H-NMR spectrum of compound **19** in Figure 21. It is noteworthy that the doublet signals are only apparent in the ^{1}H NMR spectrum after addition of one TFA drop into the NMR tube, in order to shift the water peak towards the low field region.

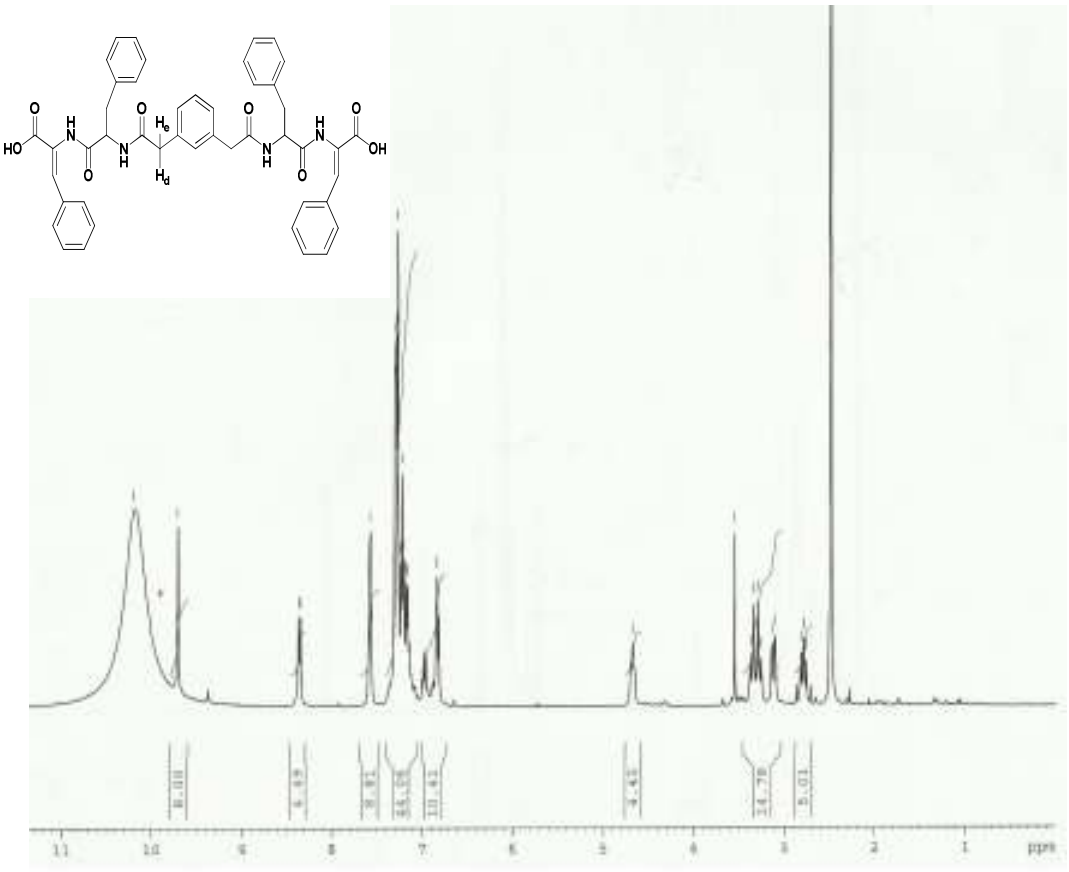

Figure 21 ^{1}H NMR (400 MHz, DMSO) spectrum for compound **19** with added TFA.

3.4. Attempt to synthesize the catechol-containing compounds 25 and 27.

The phenolic groups of caffeic acid and dihydrocaffeic acid were acetylated to avoid undesirable side reaction during the synthetic route. The next step was to activate the carboxylic acid group through the same procedure used for the synthesis of the compound **11**, using $SOCl_2$ and DMF as catalyst under a 80°C reflux for 4h. The correspondent acyl chlorides were taken without any purification and coupled with **8b.** These steps are shown in Scheme 11 and the spectra of the compounds **24** and **26** are shown in Figure 22 and 23, respectively.

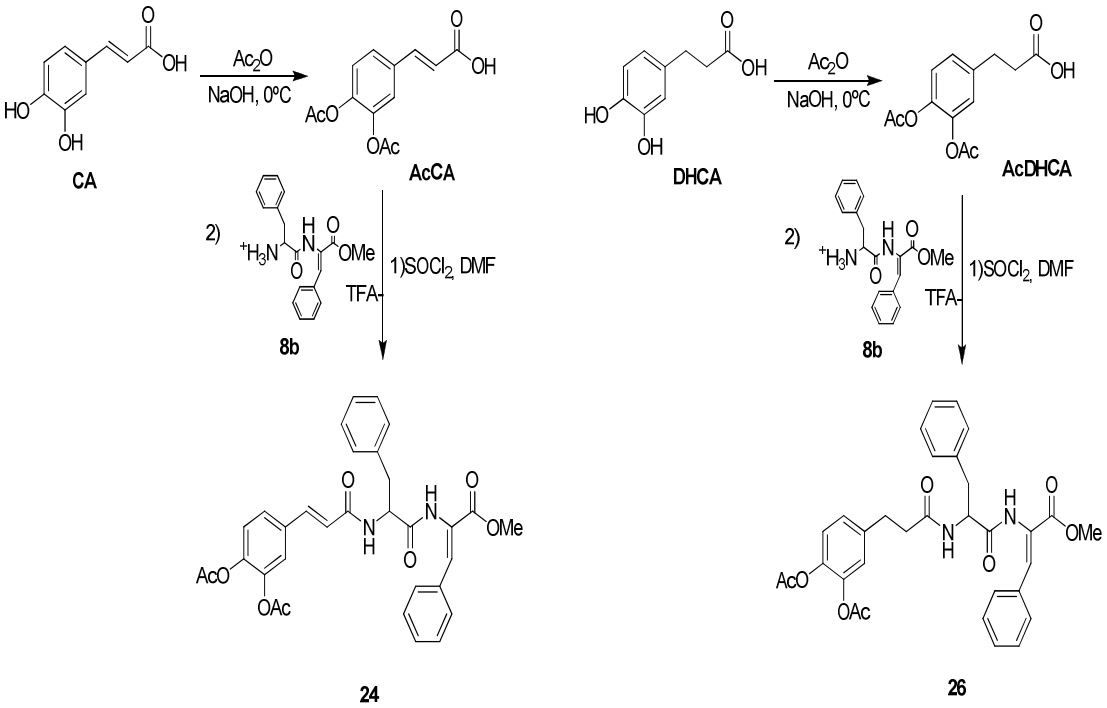

Scheme 11 Synthetic route for the coupling of dehydropeptide **8b** with caffeic acid (CA) and dihydocaffeic acid (DHCA) leading to the compounds **24** and **26**.

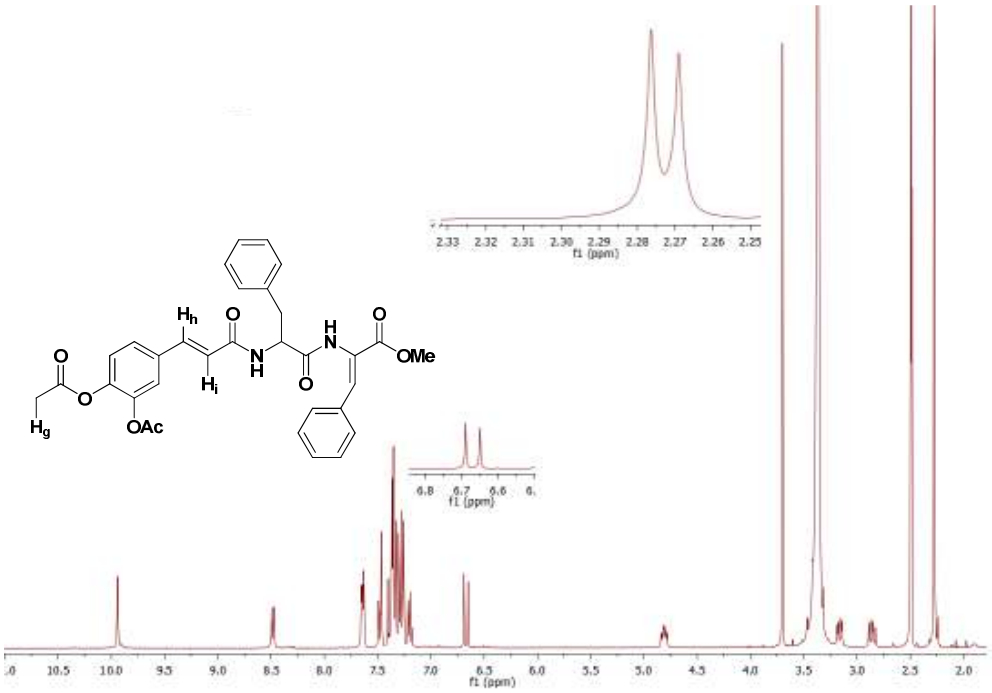

Figure 22 [1]H-NMR (400 MHz, DMSO) spectrum for compound **24**.

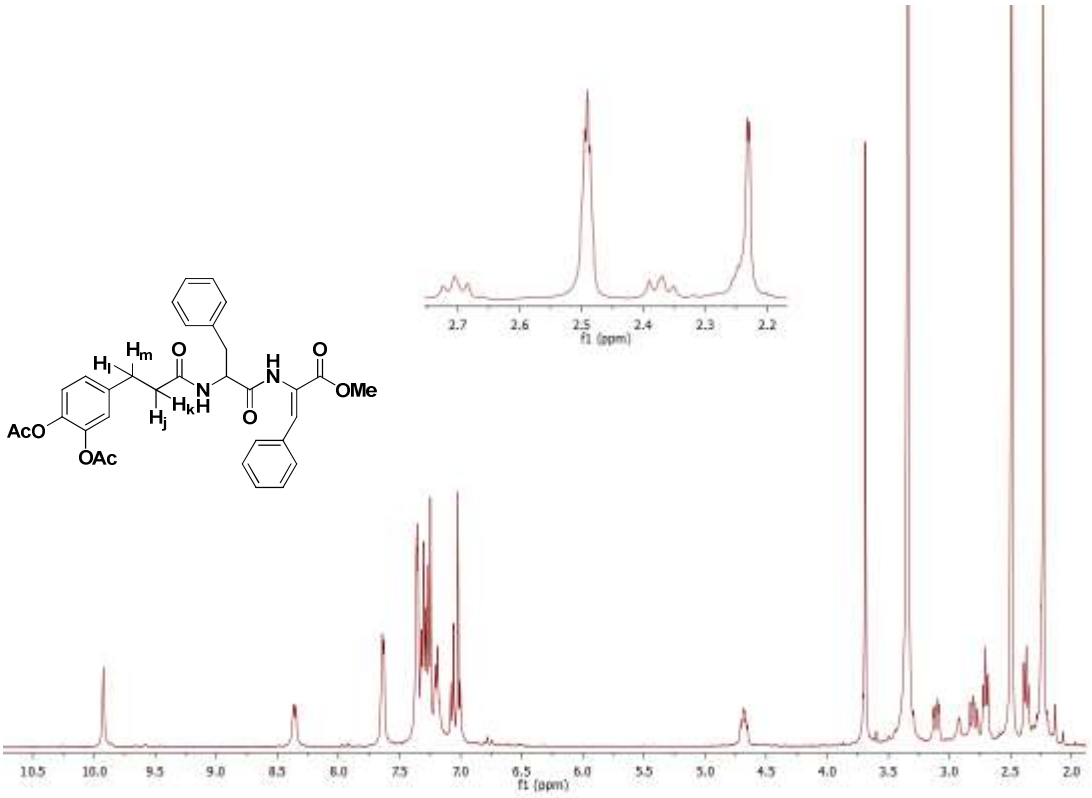

Figure 23 ^{1}H NMR (400 MHz, DMSO) spectrum for compound **26**.

Besides the characteristic signals assigned to the dehydopeptide moiety, the ^{1}H-NMR spectrum of the caffeic acid derivative (**24**) displays signals assigned to the **H_i proton** at 6.67 ppm and to the **H_h proton** within the aromatic region. The protons **H_g** of the acetyl motif are found as singlets at 2.28 and 2.27 ppm.

The ^{1}H-NMR spectrum of the dihydrocaffeic derivative (**26**) shows that the couplings constants between the diasterotopic protons **H_j** and **H_k** or **H_l** and **H_m** are too small to be seen giving give rise to two sets of triplets with a coupling constant of 7.9 Hz.

The final step on the synthetic sequence involved alkaline cleavage of the acyl protecting groups on the catechol moieties and of the methyl ester group using NaOH and dioxane. High resolution mass spectrometry analysis of the hydrolysis products of compounds **24** and **26** showed that besides the expected mass for target molecules **25** (m/z = calcd. for $C_{27}H_{24}N_2O_6$ 472.1634; found 473.1707 [M + 1]) and **27** (m/z = calcd. for $C_{27}H_{26}N_2O_6$ 474.1791; found 475.1864 [M + 1]), many more peaks displaying higher m/z values are apparent as clusters, strongly suggesting that polymerization

could have occurred during alkaline deprotection for both compounds **24** (Figure 24) and **26 (**Figure 25). Milder deprotection conditions were tested, consisting of a weaker base, K_2CO_3 in a mixture of 1:1 MeOH:CH_2Cl_2. Again, extensive polymerization was also observed.

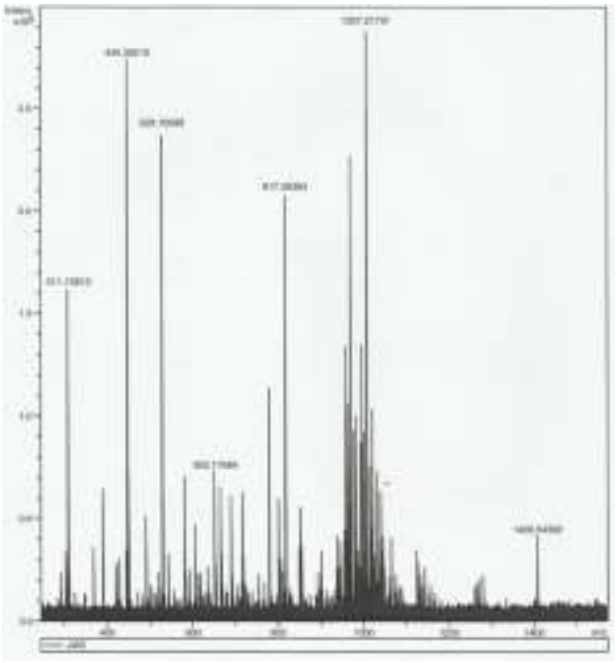

Figure 24 HRMS (ESI positive ionization) for the product obtained in the hydrolysis of compound **24**.

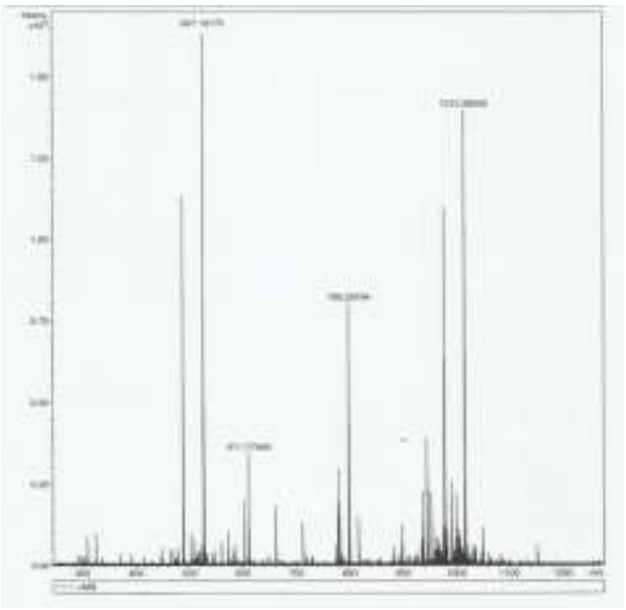

Figure 25 HRMS (ESI, positive ionization) for the product obtained in the hydrolysis of the compound **26.**

3.5. Hydrogel preparation

Hydrogels were prepared by solubilizing the dehydropeptides in water by adding small amounts of aqueous 0.5 M NaOH. Next, the pH of solution was adjusted with aqueous 0.1 M HCl until reaching the gelation point. The material was considered at the hydrogelating point when the solution viscosity increased to the point where there was no more fluid movement and the vial could be inverted without material flow.

Given the lack of purity of the CA and DHCA derivatives (**25** and **27**, respectively), these compounds were not assessed as hydrogelators. .

Compound **17a** precipitates, under these conditions, rather than forming a hydrogel network. Compound **18b** reached only the consistency of a soft gel and precipitation occurred as the concentration of this peptide was increased. The critical gelation concentration (cgc) for the prepared hydrogels is sumarized in Table 2. The structure of the successful hydrogelators is shown in Figure 26.

Table 2 Critical gelation concentration (wt%) and the pH of the resulting hydrogels.

Compound	wt%	pH
17b	0,7	6,3
18a	0,8	6,0
19	0,3	6,2
20a	0,6	6,5
20b	0,7	6,9

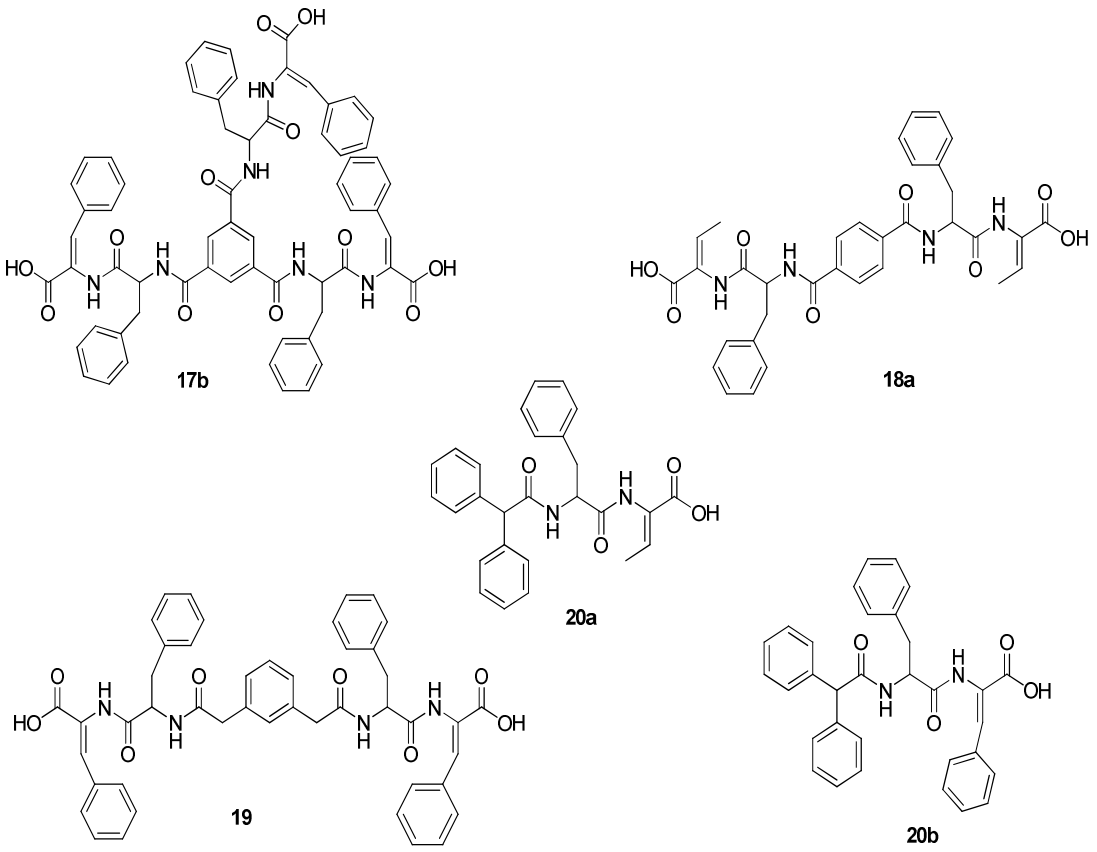

Figure 26 Structures of the modified peptides that were hydrogelators under the tested conditions.

Compound **19** emerges as the most effective hydrogelator amongst all the tested compounds. This can probably be ascribed to the additional degree of freedom introduced by the methylenic (CH_2) group between the benzene ring and the dehydrodipeptide residues.

Another point to observe is that these hydrogels are pH responsive. They are soluble at high pH values, when all carboxylic acid groups are deprotonated. As the pH decreases, the aggregation starts probably due to the aromatic-aromatic interaction and because of the arising hydrogen bonds.

It was also noticed that heating the modified dehydodipeptides accelerated the precipitation process. As the temperature was raised, the peptides started to precipitate rather than dissolving, both in distilled water (pH 7) or in phosphate buffer (10 mM , pH 6 and pH 8) . The prepared hydrogels are shown in Figure 27. The criterion to identify

the gelation point was the absence of flow, when the vials containing the materials were turned upside down.

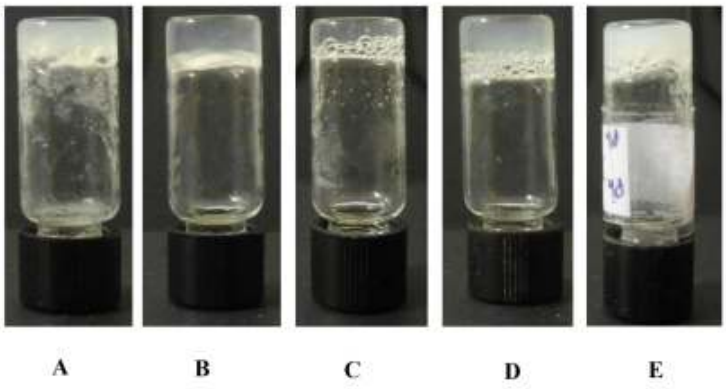

Figure 27 Hydrogels formed by hydrogelators **17b** (A), **18a** (B), **19** (C), **20a** (D) and **20b** (E).

3.6. Characterization of the hydrogels

3.6.1. Scanning transmission electron microscopy (STEM)

Scanning transmission electron microscopy (STEM) is a powerful imaging technique, useful to atomic resolution analysis. Its high sensitivity makes it suitable for the characterization of nanomaterials. It works on the same principle as the scanning electron microscopy technique (SEM): there is a focused beam of electrons that scans over the sample while some desired signal is collected to form an image. The difference with SEM is that thinner specimens are used, so that transmission modes of imaging are also available. Although the need to thin bulk materials down (until reaching electron transparency) can be a major task, this is often unnecessary for nanostructured materials. With nanomaterials the preparation requires nothing else than simply sprinkling or distributing the nanostructures onto commercially available thin cupper or

carbon support films. Grinding, polishing, or ion milling are not required, making STEM a rapid and efficient mean for nanostructure characterization.[88]

STEM technique was used to investigate the supramolecular self-consistent hydrogels formed by compounds **17b**, **18a**, **19**, **20a** and **20b**. Compounds **17b**, **20a** and **20b** resulted in hydrogels with matrices composed of fibrous networks. These hydrogels exhibited fibers with diameters in the order of 28±10 nanometer and lengths in the micrometer scale. These characteristics lead to high surface to volume ratios which possibly guarantee suitable water swelling properties to the material. Hydrogel **17b** generated shorter fibers, which could impact on its rheological properties, mainly on the storage modulus value. The micrograph of hydrogel **18a** shows flat ribbons, which probably result from fiber aggregation processes. The STEM images are shown in Figure 28.

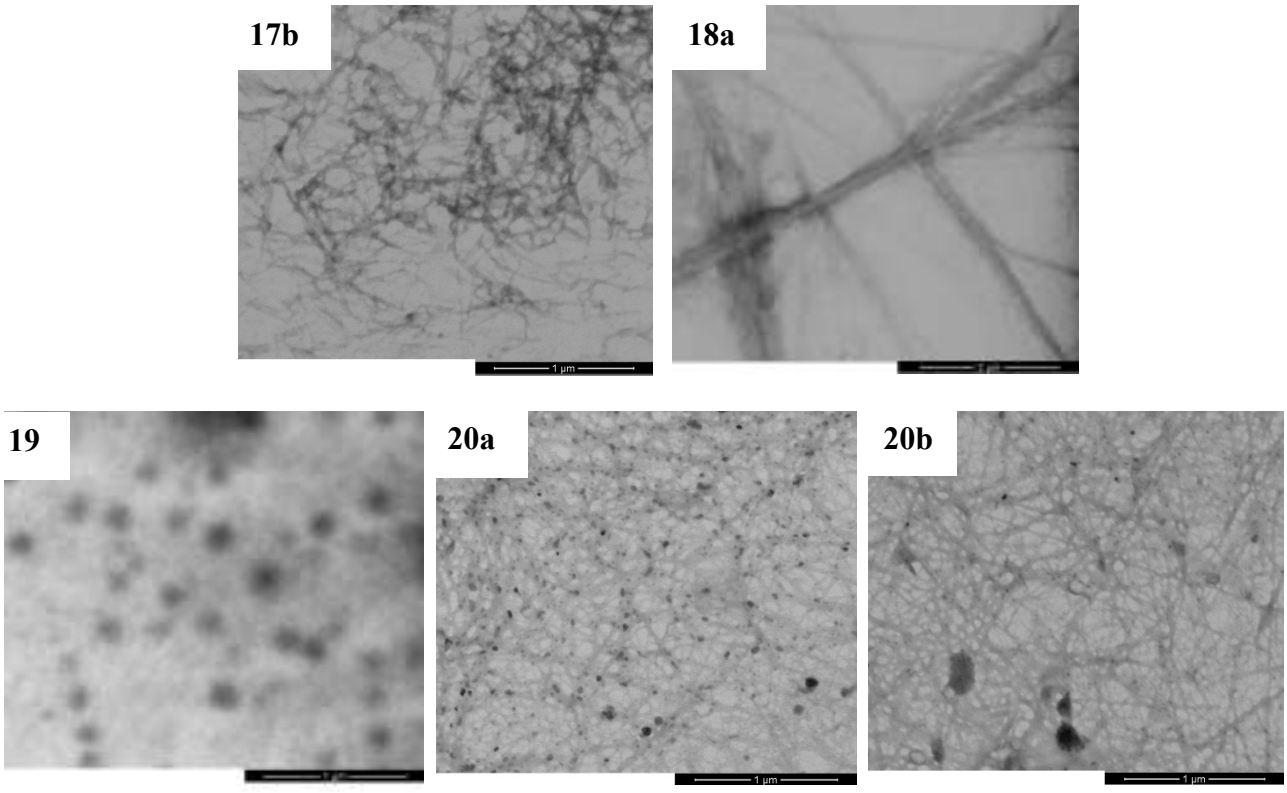

Figure 28 STEM images of the hydrogels formed by compounds **17b**, **18a**, **19**, **20a** and **20b**.

The hydrogel of compound **19** resulted in spherical aggregation patterns under the experimental conditions used for gel formation. This is in accordance to the work of Reches *et al*. with other N-modified aromatic dipeptide hydrogelators.[89] In Scheme 12 is depicted a schematic representation of a hypothetical hierarchical self-assembly process of hydrogelators leading to formation of spheres.

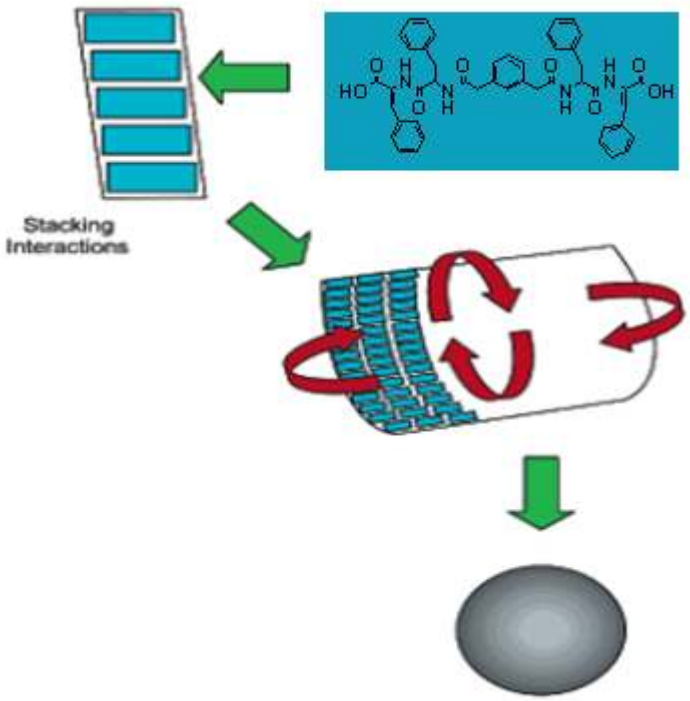

Scheme 12 Representation of the spherical packing hypothesis for compound **19**. The formation of spheres may result from closure of the sheet along two axes. Picture adapted from Reference 89 [89].

However, this kind of interpretation have to be further investigated, mainly because the nanostructure morphology can be controlled by many experimental parameters such as the dilution or the kinetics involved in the formation of the nanostructures.

The concentration dependent structural transitions in the peptide-based building blocks have been confirmed[90, 91]: for example, the conversion between tubular and spherical nanostructures of the self-assembling dipeptide H-Phe-Phe-NH_2·HCl is susceptible of being readily modulated by varying the concentration of the peptide

building blocks as is shown in Figure 29[92]. This is demonstrated in micrographs acquired by atomic force microscopy AFM (a and b), fluorescent optical image (c) and TEM. It is noticeable that spheres in a necklace-like structure are formed as an intermediate state between the nanotubes or nanospheres into vesicle-like structures.

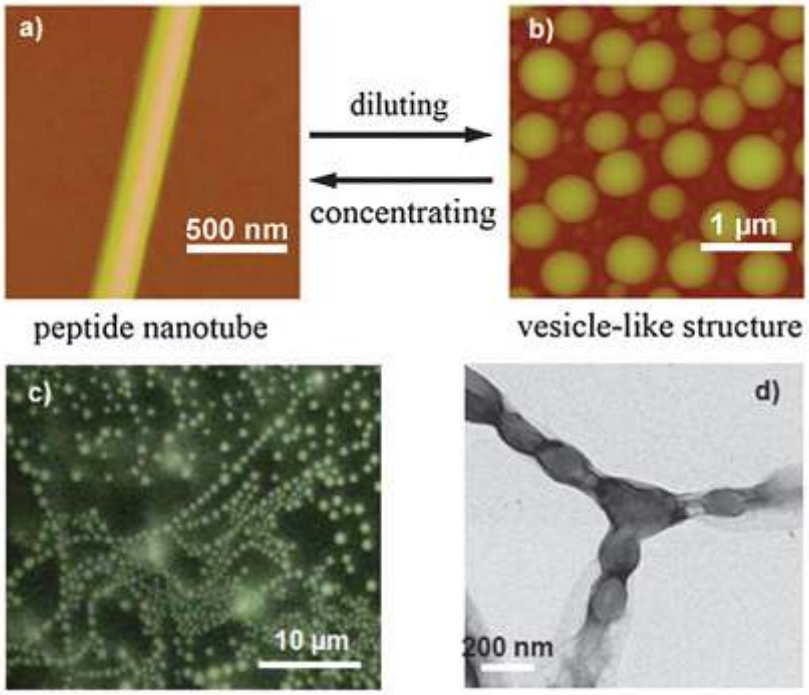

Figure 29 Reversible transition between peptide nanotubes and vesicle-like structures: AFM height image of nanotubes (a) and vesicle-like structures (b). (c) Fluorescent optical image of the joined necklace-like structures composed of spherical vesicles bound with fluorescently-labeled ss-DNA and (d) TEM image of the joined necklace-like structures[92].

3.6.2. Circular dichroism analysis

A circular dichroism study was undertaken, to ascertain the presence of structured patterns in solution below critical gelation concentration, for the hydrogelators **17b**, **18a**, **19**, **20a** and **20b**. Solutions of hydrogelators **17b**, **18a**, **19**, **20a** and **20b (**0.2 mg/mL) at the corresponding gelation pH (Table 2) were prepared in a 10 mM phosphate buffer. CD spectra are shown in Figure 30 (A-C). Spectra were normalized and subjected to a 3-point smoothing.

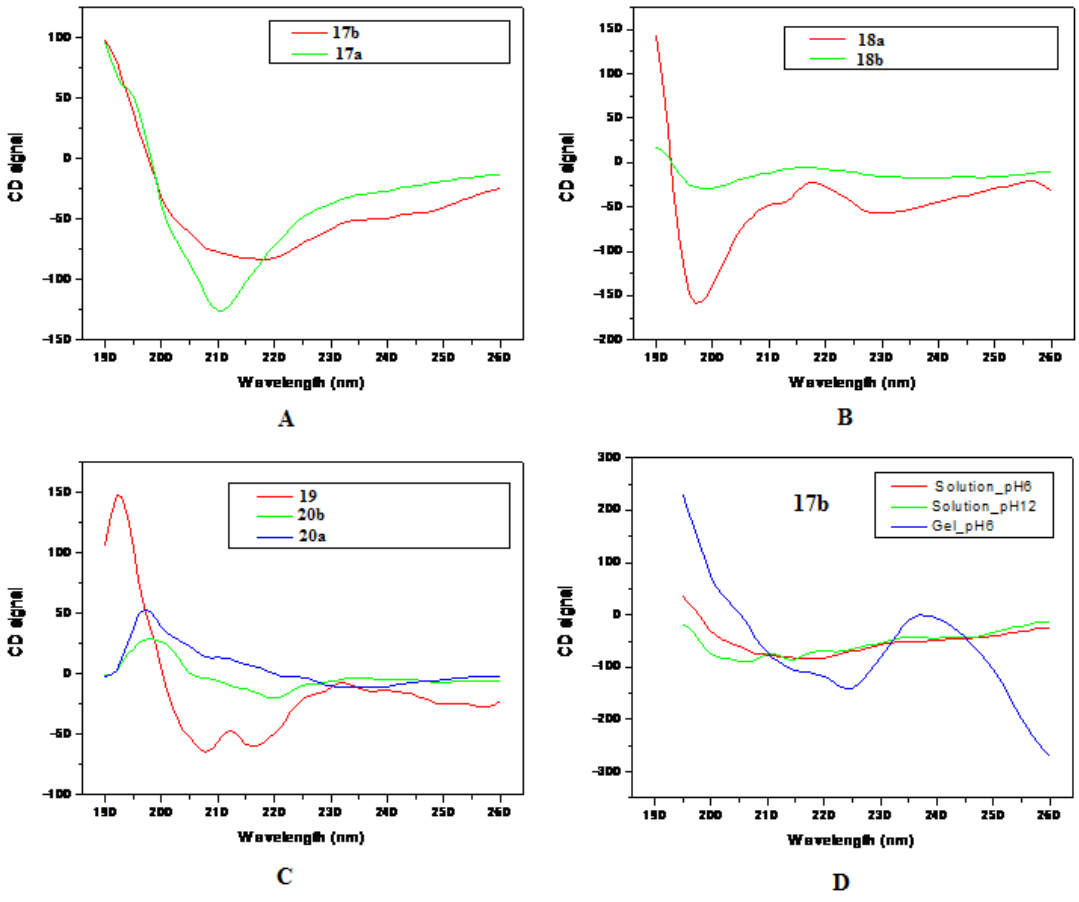

Figure 30 CD spectra of: (A) hydrogelators **17a** and **17b**; (B) hydrogelators **18a** and **18b**; (C) hydrogelators **19**, **20a** and **20b**; (D) Hydrogelator **17b** at pH 6 (red), hydrogelator **17b** at pH 12 (green), hydrogel of compound **17b** (blue).

CD spectra were acquired in the wavelength range 195-260 nm. In this spectral window, CD signals resulting mainly from absorbances of the peptide bonds, are expected.

Compound **17a** shows the CD amide absorption (around 210 nm), at a lower wavelength than compound **17b** (215 nm) suggesting that, under these experimental conditions, non-hydrogelating compound **17a** displays less ordered structures in solution than hydrogelator **17b**. Based on the shape of its spectra, compound **17b** seems to have propensity for aggregating into β-sheets.

The CD spectrum for hydrogelator **18a** shows that the concentration used in this experiment is insufficient to produce any aggregation pattern. This could reflect the fact that this hydrogelator displays the highest critical gelation concentration (0.8%).

On the other hand, compound **19**, which displays the lowest cgc (0.3%), showed strong evidence of aggregating into an α-helical pattern. As expected, compound **18b**, which failed to form hydrogel, does not shows evidence of any organized structures.

The CD spectra of the compounds **20a** and **20b** show an amide absorption in the wavelength range from 205 to 220 nm suggesting the presence of some kind of pre-organized nanostructures in solution, probably β-sheet packing, under this set of experimental conditions.

Besides these experiments, compound **17b** was also evaluated at its cgc, as gel, and at pH 12 (Fig. 26 D). The hydrogel **17b** was adjusted to pH 12 by treatment with aqueous NaOH 1 M, resulting in a solution of **17b** at a concentration similar to its cgc. According to these data, we can infer that at basic pH there are no pre-organized structures. This is in accordance to the fact that at pH 12 the hydrogelator molecules are mostly deprotonated. In these conditions electrostatic repulsion prevails making hydrogelator molecules more prone to aqueous solvation rather than undergoing self-assembly. The CD spectrum for the hydrogel of **17b** reveals the presence of more organized structures possibly self-assembly into a β-sheet pattern.

4. Conclusions and Future Perspectives

In this work we have synthesized a small library of novel chemically diverse N-dehydrodipeptides designed as novel hydrogelators. The ability of the members of the library to form hydrogels was evaluated. It was found that five, out of seven compounds tested, were able to self-assemble into a water swelling network giving self-consistent pH-controlled hydrogel materials. STEM microscopy revealed that the hydrogels are composed of fibers, ribbons and even spheres. The results also suggest that a spacer between the organic modifier and the dipeptide moiety could lead to lower cgc´s.

The preliminary CD study, that was performed to ascertain the degree of organization of the hydrogelator molecules, suggested that at extremely high pH, there are no pre-organized structures and the hydrogelators presented some kind of organizational pattern in the tested conditions, specially the compound **19** probably due to its lowest cgc. The non-hydrogelating ones didn´t show any ordered pattern.

Mechanical characterization, which can elucidate the rheological behavior of the hydrogels and a deeper investigation of their supra-molecular organization are essential to direct the use of these hydrogels into new devices.

A future perspective for this work is to combine the experimental data developed around the synthesized molecules with molecular modeling techniques, especially molecular dynamics, in order to have more insight into the understanding about the driving forces involved in the self-assembly process of these low molecular weight hydrogelators.

5. Experimental Section

All the reagents were commercially acquired with a high level of purity and were used without any kind of pre-treatment.

Melting points (ºC) were determined in a Gallenkamp apparatus and are uncorrected. ^{1}H and ^{13}C-NMR spectra were recorded on a Varian Unity Plus at 300 and 75.4 MHz, respectively or on a Bruker Avance II+ at 400 and 100.6 MHz, respectively. ^{1}H-^{1}H spin-spin decoupling, bidimensional NMR techniques (HMBC, HSQC) and DEPT θ 45º were used. Chemical shifts are given in ppm and coupling constants in Hz. MS and HRMS data were recorded by the mass spectrometry service of the University of Vigo, Spain; elemental analysis was performed on a Leco CHNS 932 elemental analyser.

The reactions were monitored by thin layer chromatography (t.l.c.) in Merck-Kieselgel 60 F254 plates. T.l.c were revealed with an UV lamp (ν = 50 Hz) in a UV chamber CN-6 or with iodine. Column chromatography was performed on silica gel MN Kieselgel 60 M 230-400 mesh. Petroleum ether refers to the boiling range 40-60 ºC. When solvent gradient was used, the increase of polarity was made from neat petroleum ether to mixtures of ethyl acetate/petroleum ether, with increasing steps of 10% of ethyl acetate, until the isolation of the product was accomplished.

The dry toluene was commercially acquired and the DCM, acetonitrile and THF were dried using the standards procedures described in Vogel's Textbook of Practical Organic Chemistry[93]. Briefly, DCM was, at first, treated with calcium chloride ($CaCl_2$) and calcium hydride (CaH_2) and then distillated. The acetonitrile was treated with silica and calcium hydride (CaH_2), distilled and stored with molecular sieves. The THF was mixtured with thin slices of metallic sodium for 24 hours and next it was refluxed with benzophenone until the media got in a blue-purple color. Next, it was distilled and stored with molecular sieves.

The hydrogel preparation was accomplished by weighting the appropriate amount of the final modified dipeptides into 2 mL glass vials and then 300μL of distilled water was added. The samples were submitted to sonication for 60s. Next, drops of 10 μL of a NaOH 0,5 M solution was added until the suspended solid was completely dissolved. In

this step, a vortex was used to mix the system more efficiently. Then, drops of 10 μL of HCl 0,1M solution were added, carefully and followed by mixing, until media reach the gelation point. The final pH values were estimated by putting a spatula tip of the hydrogel onto a tape of universal indicator paper and then this pH values were précised using a Crison Micro TT 2050 pHmeter.

The STEM analysis was performed using the microscopy service of the University of Minho (Guimarães) and the CD spectra were recorded in the University of Coimbra.

5.1. Synthesis of dehydroamino acid derivatives 8a and 8b.

5.1.1. Synthesis of H-L-Thr-OMe·HCl (3a):

A 250 mL reaction flask containing methanol (1ml/mmol of aa, 50mL) was cooled with an ice bath and then $SOCl_2$ (3.4 eq., 170 mmol, 42.5 ml) was added, drop-wise, under stirring. Next, the H-L-Thr-OH (50 mmol, 5.96 g) was slowly joined and the reaction was kept under a 40°C reflux for 4 hours. Then the solvent was evaporated and resulted in an transparent oil with 80% yield. It was not possible to crystallize the product.

^{1}H-NMR (400 MHz, DMSO): δ = 1.19 (d, 3H, J= 6.6 Hz, CH_3); 3.72 (s, 3H, OCH_3); 3.89 (m, 1H, β-CH); 4.10 (m, *J* = 6.6, 3.9 Hz, 1H, α-CH); 5.02 (br s, 1H, β-OH); 8.53-8.47 (m, 3H, $NH3^+$).

5.1.2. Synthesis of H-DL-Phe(β-OH)-OMe·HCl (3b):

A 250 mL reaction flask containing 50 mL of methanol (1mL/mmol of the a.a) was cooled with an ice bath and then $SOCl_2$ (3.4 eq., 170 mmol, 42.5 mL) was added, drop-wise, under stirring. Next, the H-DL-Phe(β-OH)-OH (50 mmol, 9.06g) was slowly

joined and the reaction was kept under a 40°C reflux for 4 hours. Then the solvent was evaporated and the resulting material was recrystallized from methanol/diethyl ether. A white solid with 100% yield was obtained.

^{1}H-NMR (400 MHz, DMSO): δ = 3.60 (s, 3H, OCH3); 4.13 (d, 1H, J = 5.6 Hz; α-CH); 5.01 (d, 1H, J = 5.6 Hz; β-CH); 6.60-6.53 (br s, 1H, β-OH); 7.31-7.40 (m, 5H, H-Ar); 8.50 (br s, 3H, $NH3^+$).

5.1.3. Synthesis of Boc-L-Phe-OH[94] (4):

L-Phe-OH (50 mmol; 8.26 g) was dissolved in a mixture of dioxane (100 mL), water (50 mL) and a solution of NaOH 1M (1.0 eq., 50 mmol, 50 mL) under vigorous stirring. The system was cooled with an ice bath and then Boc_2O (1.1 eq., 55 mmol, 12.00 g) was added. After stirring at room temperature for 4 hours, the dioxane was evaporated and the resulting material was cooled in a water bath. Ethyl acetate (100 mL) was added to the reaction vial and the pH was adjusted to 2 by using a solution of $KHSO_4$ 1M (60 mL). The aqueous phase was extracted with ethyl acetate (2x 30 mL). All the organic phases were gathered and washed with water (2x 30 mL), dried over $MgSO_4$ and evaporated under reduced pressure to give transparent oil that was crystallized in ethyl acetate/hexane giving a white solid with quantitative yields.

^{1}H-NMR (300 MHz, DMSO): δ = 1.306 (s, 9H, $C(CH_3)_3$); 2.850-2.770 (dd, 1H, J = 10.2 and 13.7 Hz; β-CH_2); 2.976-3.037 (dd, 1H, J = 4.5 and 13.7 Hz; β-CH2); 4.091 (m, 1H, α-CH); 7.064-7.091 (d, 1H, J = 8.1Hz; N-H); 7.161-7.291 (m, 5H, H-Ar); 12.60 (br s, 1H, OH).

5.1.4. Synthesis of Boc-L-Phe-L-Thr-OMe (5a):

Boc-L-Phe–OH (1.0 eq., 12.1 mmol, 3.2 g) was dissolved in acetonitrile (30 mL) and immersed in an ice bath. HOBt (1.0 eq., 12.1 mmol, 1.64 g), DCC (1.2 eq., 14.5 mmol, 3.0 g), H-L-Thr-OMe (1.0 eq., 12.1 mmol, 2.05 g) and triethylamine (2.0 eq., 24.2 mmol, 3.37 mL) were added, waiting about 2 minutes between each addiction. The mixture was left stirring overnight. Next, the reaction was filtered to exclude the DCU (dicyclohexyl urea) and the liquid was evaporated under reduced pressure. Then 60 mL of acetone was added and the flask was stored in the freezer for 3 hours to precipitate more DCU. So the reaction is filtered again and the liquid was evaporated again. To the resulting yellow oil 80 mL of ethyl acetate was added and this organic phase was washed successively with aqueous $KHSO_4$ 1M (3x 30 ml), $NaHCO_3$ 1M (3x 30 mL) and saturated NaCl (3x 30 ml) solutions. The organic phase was dried over anhydrous $MgSO_4$ and the solvent removed in vacuum. The compound **6a** was obtained as 52%.

^{1}H-NMR (400 MHz, $CDCl_3$): δ = 1.150-1.172 (d, 3H, 6.6 Hz; CH_3); 1.391 (s, 9H, $C(CH_3)_3$); 2.987-3.057 (dd, 1H, J = 13.7 and 6.3 Hz; β-CH_2); 3.108-3.175 (dd, 1H, J= 13.7 and 6.3 Hz; β-CH_2); 3.719 (s, 3H, OCH_3); 4.287 (br s, 1H, β-CH); 4.390-4.460 (m,1H, α-CH); 4.563-4.602 (dd, 1H, J = 6.3 and 9.0 Hz; α-CH); 5.160-5.185 (d, 1H, J= 7.5 Hz; N-H); 6.881-6.911 (d, 1H, J= 9.0 Hz; N-H); 7.208–7.284 (m, 5H, H-Ar).

5.1.5. Synthesis of Boc-L-Phe-DL-Phe(β-OH)-OMe (5b):

Boc-L-Phe–OH (1.0 eq., 12.3 mmol, 3.3 g) was dissolved in acetonitrile (30 mL) and immersed in an ice bath. HOBt (1.0 eq., 12.3 mmol, 1.66 g), DCC (1.2 eq., 14.7 mmol, 3.04 g), H-DL-Phe(β-OH)-OMe (1.0 eq., 12.3 mmol, 2.84 g) and triethylamine (2.0 eq., 24.6 mmol, 3.42 mL) were added, waiting about 2 minutes between each addiction. The mixture was left stirring overnight. Next, the reaction was filtered to exclude the DCU (dicyclohexyl urea) and the liquid was evaporated under reduced pressure. Then 60 mL of acetone was added and the flask was stored in the freezer for 3 hours to precipitate

more DCU. So the reaction is filtered again and the liquid was evaporated again. To the resulting yellow oil 80 mL of ethyl acetate was added and this organic phase was washed successively with aqueous $KHSO_4$ 1M (3x 30 ml), $NaHCO_3$ 1M (3x 30 mL) and saturated NaCl (3x 30 ml) solutions. The organic phase was dried over $MgSO_4$ anhydrous and the solvent removed in vacuum. The compound **6a** was obtained as a diasteroisomeric mixture with a 78% yield.

^{1}H-NMR (400 MHz, $CDCl_3$): δ = 7.33-7.23 (m, 10 H, H-Ar), 7.04 (dd, *J* = 7.3, 1.9 Hz, 1H), 6.87 and 6.71 (d, *J* = 8.8 Hz, 1H), 5.24 – 5.17 (br s, 1H, OH), 4.93 – 4.81 (m, 1H, α H Phe), 4.33-4.36 (m, 1H, α H Phe (β-OH)), 3.68 and 3.71 (s, 3 H, OCH3), 3.19 (d, *J* = 4.2 Hz, 1H, β H Phe (β-OH)), 3.09 – 2.96 (m, 1H, β H Phe), 2.92 – 2.85 (m, 1H, β H Phe), 1.40 (s, 9H, $C(CH_3)_3$).

5.1.6. Synthesis of Boc-L-Phe-ΔAbu-OMe (7a):

Boc-L-Phe-(L)-Thr-OMe (6.21 mmol, 2.36 g) was dissolved in 15 mL of dry acetonitrile and the. DMAP (0.11 eq, 0.68 mmol, 0,083g), Boc_2O (1.1 eq., 6.83 mmol, 1.49g) were added under stirring at room temperature. The reaction flask was sealed with a $CaCl_2$ tube and the synthesis has been followed by ^{1}H-NMR. After proving that the initial material was converted to Boc-L-Phe-L-Thr-(β-Boc)-OMe, TMG (0,02 mL/mL of solvent; 0,3 mL) was joined to the reaction. After 24 hours there was evidence, by ^{1}H-NMR, that all the material was converted into the product **7a**. The solvent was evaporated and the orange resulting oil was dissolved in ethyl acetate (80 ml). This organic phase was washed successively with aqueous $KHSO_4$ 1M (3x 30 ml), $NaHCO_3$ 1M (3x 30 mL) and saturated NaCl (3x 30 ml) solutions. The organic phase was dried over anhydrous $MgSO_4$ and the solvent removed in vacuum. A yellow solid (1.52 g; 71%) was obtained.

^{1}H-NMR (400 MHz, $CDCl_3$): δ = 7.37-7.21 (m, 6H, H-Ar), 6.80 (q, *J* = 7.2 Hz, 1H, β H ΔAbu), 5.00 (br s, 1H, α NH Phe), 4.48 (m, 1H, α NH Phe), 3.74 (s, 3H, OCH_3), 3.16-3.21 (dd, 1H, J = 14.0 and 6.4 Hz, β H Phe), 3.06-3.11 (dd, 1H, J = 14.0 and 7.2 Hz, β H Phe), 1.70 (d, *J* = 7.2 Hz, 3H, β CH_3 ΔAbu), 1.43 (s, 9H, $C(CH_3)_3$) ppm.

5.1.7. Synthesis of Boc-L-Phe-ΔPhe-OMe (7b):

The procedure described above was followed with compound **6b** (9.32 mmol; 4.12 g) giving the product **7b** (86%; 2.90 g) as a yellow solid.

^{1}H-NMR (400 MHz, $CDCl_3$): δ = 7.67 (s, 1H, α NH ΔPhe), 7.42-7.21 (m, 11H, H-Ar + β H ΔPhe), 5.01-4.94 (m, 1H, α NH Phe), 4.14 – 4.06 (m, 1H, α H Phe), 3.83 (s, 3H, OCH_3), 3.21 (dd, *J* = 14.0, 6.6 Hz, 1H), 3.08 (dd, *J* = 14.0, 7.2 Hz, 1H), 1.41 (s, 9H, $C(CH_3)_3$) ppm.

5.1.8. Synthesis of H-L-Phe-Z-ΔAbu-OMe,TFA (8a):

Boc-(L)-Phe-ΔAbu OMe **, 7a,** (4.8 mmol, 1.74 g) was dissolved in TFA (3 mL/mmol; 14.4 mL) and the reaction stayed under stirring for 3 hours when there was evidence, by following the process with TLC (with ethyl acetate as eluent), that all the reactant **7a** had been consumed, giving the compound **8a** (87 %, 1.56 g) as an yellow oil.

^{1}H-NMR (400 MHz, DMSO): δ = 1.60 (d, 3 H, *J* = 7.2 Hz, γCH_3 ΔAbu), 2.99-3.05 (dd, 1 H, *J* = 14.0 and 8.0 Hz, βCH_2), 3.14-3.19 (dd, 1 H, *J* = 14.0 and 6.0 Hz, βCH_2 Phe), 3.66 (s, 3 H, OCH_3), 4.18-4.20 (m, 1 H, αCH Phe), 6.60 (q, 1 H, *J* = 7.2 Hz, βCH ΔAbu), 7.27-7.34 (m, 5 H, HAr), 8.29 (s br, 3 H, αNH_3^+), 9.89 (s, 1 H, αNH ΔAbu) ppm.

^{13}C-NMR (100.6 MHz, DMSO): δ = 13.45 (γCH_3 ΔAbu), 37.04 (βCH_2 Phe), 52.00 (OCH_3), 53.41 (αCH Phe), 126.71 (αC), 127.22 (CH), 128.57 (CH), 129.57 (CH), 133.68 (βCH ΔAbu), 134.74 (C), 164.11 (C=O), 167.22 (C=O) ppm. HRMS (micrOTOF): calcd. for $C_{14}H_{19}N_2O_3$ 263.13902; found 263.13925.

5.1.9. Synthesis of H-L-Phe-*Z*-ΔPhe-OMe,TFA (8b):

The general procedure described above was followed using compound **7b** (1.95 mmol, 0.862 g) giving compound **3a** (92 %, 0.79g) as a white solid, m.p. 87.0-88.0ºC.
^{1}H-NMR (400 MHz, DMSO): δ = 2.94–3.00 (dd, 1 H, *J* = 14.0 and 8.8 Hz, βCH$_2$ Phe), 3.24–3.29 (dd, 1 H, *J* = 4.8 and 14.0 Hz, βCH$_2$ Phe), 3.73 (s, 3H, OCH$_3$), 4.25 (m, 1H, αCH Phe), 7.30–7.41 (m, 9 H, ArH and βCH ΔPhe), 7.58-7.60 (dd, *J* = 2.0 and 4.0 Hz, 2 H, ArH), 8.26 (s br, 3 H, NH_3^+), 10.37 (s, 1 H, NH ΔPhe) ppm.
^{13}C-NMR (100.6 MHz, DMSO): *δ* = 36.69 (βCH$_2$ Phe), 52.37 (OCH$_3$), 53.61 (αCH Phe), 125.03 (αC), 127.31 (CH), 128.64 (CH), 128.71 (CH), 129.57 (CH), 129.72 (CH), 130.01 (CH), 132.31 (βCH ΔPhe), 132.83 (C), 134.80 (C), 164.87 (C=O), 168.30 (C=O) ppm. HRMS (micrOTOF): calcd. for $C_{19}H_{21}N_2O_3$ 325.15467; found 325.15545.

5.2. Coupling of the dehypeptides to the organic modifiers.

5.2.1. Synthesis of compound 13a:

To a stirred solution of trimesoyl chloride (72 mg, 0.27 mmol) in dry THF (5 mL), triethylamine (7.0 eq., 1.89 mmol, 0.27 mL) was added and then H-L-Phe-*Z*-ΔAbu-OMe,TFA**, 8b,** (3.5 eq., 0.95 mmol, 357.2 mg) was added under nitrogen atmosphere. This mixture was stirred for 1 h at room temperature and then refluxed for 48 h under 80°C. The reaction was filtered; the solid was, separately, washed with water and proved to be just Et_3NHCl (because the entire solid was dissolved in water). The filtered organic THF phase was evaporated and 50 mL of CH_2Cl_2 was added to the resultant material. This organic solution was successively washed with aqueous $KHSO_4$ 1M (2x 10 ml), $NaHCO_3$ 1M (2x 10 mL) and Brine (2x 10 ml) solutions. The organic phase was dried over anhydrous $MgSO_4$ and the solvent removed under reduced pressure. In order to crystallize the material, 30 mL of ethyl acetate was added and this suspension was stored in the freezer for 24h. The suspension was filtered and the compound **13a** was obtained as a white solid that was washed with ethyl ether and dried under vacuum. Yield: 52%; mp: 231 – 233°C.

^{1}H-NMR (400 MHz, DMSO-d_6): δ = 1.646-1.664 (d, 9 H, *J* = 7.2 Hz, γCH_3 ΔAbu), 3.037-3.097 (dd, 3 H, *J* = 13.6 and 10.4 Hz, βCH_2), 3.162- 3.206 (dd, 3 H, *J* = 4.4 and 13.6 Hz, βCH_2 Phe), 3.632 (s, 9 H, OCH_3), 4.901-4.908 (m, 3 H, αCH Phe), 6.552-6.570 (q, 1 H, *J* = 7.2 Hz, βCH ΔAbu), 7.224-7.2614 (t, 3H, J=7.2 Hz, H-pAr), 7.136-7.173 (m, 6 H, H-mAr), 7.364-7.382 (d, 6 H, J= 7.2 Hz, H-oAr), 8.35 (s, 3H, H-Ar; central ring), 8.903-8.924 (d, 3H, J= 8.4 Hz, αNH Phe), 9.546 (s, 3 H, αNH ΔAbu) ppm.

^{13}C-NMR (100.6 MHz, DMSO): δ = 13.49 (γCH_3 ΔAbu), 37.26 (βCH_2 Phe), 51.85 (OCH_3), 54.91 (αCH Phe), 127.65 (αC), 126.29 (CH), 128.10 (CH), 129.19 (2 CH), 132.73 (βCH ΔAbu), 134.25 (C), 138.04 (C); 164.54 (C=O), 165.45 (C=O), 170.37 (C=O) ppm.

HRMS (ESI): calcd. for $C_{51}H_{54}N_6O_{12}$ 942.37997; found 943.39039 [M+1].

5.2.2. Synthesis of compound 13b:

To a stirred solution of trimesoyl chloride (72 mg, 0.27 mmol) in dry THF (5 mL), triethylamine (7.0 eq., 1.89 mmol, 0.27 mL) was added and then H-(L)-Phe-*Z*-ΔPhe-OMe,TFA**, 8b,** (3.5 eq., 0.95 mmol, 413.8 mg) was gathered under nitrogen atmosphere. This mixture was stirred for 1 h at room temperature and then refluxed for 48 h under 80°C The white precipitate was filtered and washed several times with cold water to remove the byproduct Et_3NHCl and finally with ethyl ether. This white solid was dried under vacuum. Yield: 46%; mp: 272 – 275°C.

^{1}H-NMR (400 MHz, DMSO-d_6): δ = 3.081-3.111 (dd, 3H, J =13.7 and 10.4 Hz, β-CH_2); 3.22-3.249 (dd, 3H, J =13.7 and 4.1 Hz , β-CH_2); 3.704 (s, 9H, OCH_3); 4.912-4.965 (m, 3H, α-CH); 7.156-7.192 (t, 3H, J = 7.2 Hz); 7.247-7.278 (m, 6H, H-Ar; Phe); 7.278 (s, 3H, β-H; ΔPhe); 7.305-7.353 (m, 9H, H-Ar; ΔPhe); 7.404-7.423 (d, 6H, J =7.6 Hz, H-Ar; Phe); 7.660-7.678 (d, 6H, H-Ar; ΔPhe); 8.402 (m, 3H, H-Ar; central ring); 8.979 (d, 3H, J = 7.6 Hz; αNH Phe); 10.006 (s, 3H, αNH ΔPhe).

^{13}C-NMR (100.6 MHz, DMSO): *δ* = 36.58 (βCH_2 Phe), 52.19 (OCH_3), 55.13 (αCH Phe), 125.97 (αC), 126.33 (CH), 128.15 (CH), 128.55 (CH), 129.18 (CH), 129.31 (CH),

129.46 (CH), 130.05 (CH), 131.97 (βCH ΔPhe), 133.22 (C), 134.33 (C), 138.14 (C), 165.34 (C=O), 165.75 (C=O), 171.38 (C=O) ppm.
HRMS (ESI): calcd. for $C_{66}H_{60}N_6O_{12}$ 1128.42692; found 1129.43155 [M+1].

5.2.3. Synthesis of compound 14a:

To a stirred solution of terephtaloyl chloride (50.75 mg, 0.25 mmol) in dry THF (5 mL), triethylamine (5.0 eq., 1.25 mmol, 0.18 mL) and H-(L)-Phe-*Z*-ΔAbu-OMe, TFA**, 8a,** (2.4 eq., 0.6 mmol, 225.6 mg) were successively added under nitrogen atmosphere. This mixture was stirred for 1 h at room temperature and then refluxed for 48 h under 80°C. The reaction was filtered; the solid was, separately, washed with water and proved to be just Et_3NHCl because of its water solubility. The filtered organic THF phase was evaporated and 50 mL of CH_2Cl_2 was added to the resultant material. This organic solution was successively washed with aqueous $KHSO_4$ 1M (2x 10 ml), $NaHCO_3$ 1M (2x 10 mL) and Brine (2x 10 ml) solutions. The organic phase was dried over anhydrous MgSO4 and the solvent was removed under reduced pressure. In order to crystallize the material, 30 mL of ethyl acetate was added and this suspension was stored in the freezer for 24h. The suspension was filtered and the compound **13a** was obtained as a white solid that was washed with ethyl ether and dried under vacuum. Yield: 67%; mp: 219 – 221°C.

^{1}H-NMR (400 MHz, DMSO-d_6): δ = 1.653-1.671 (d, 6 H, *J* = 7.2 Hz, γCH_3 ΔAbu), 3.000-3.061 (dd, 2 H, *J* = 13.6 and 10.8 Hz, βCH_2), 3.157-3.201 (dd, 2 H, *J* = 4.4 and 13.6 Hz, βCH_2 Phe), 3.638 (s, 6 H, OCH_3), 4.819-4.877 (m, 2 H, αCH Phe), 6.560-6.578 (q, 1 H, *J* = 7.2 Hz, βCH ΔAbu), 7.234-7.272 (t, 3H, J = 7.2 Hz, H-pAr), 7.138-7.175 (m, 4 H, H-mAr), 7.368-7.386 (d, 4 H, J = 7.2 Hz, H-oAr), 7.820 (s, 4H, H-Ar; central ring), 8.740 (d, 2H, J = 8.4 Hz, αNH Phe), 9.498 (s, 2 H, αNH ΔAbu) ppm.

^{13}C-NMR (100.6 MHz, DMSO): δ = 13.55 (γCH_3 ΔAbu), 37.19 (βCH_2 Phe), 51.93 (OCH_3), 54.90 (αCH Phe), 127.65 (αC), 126.36 (CH), 127.34 (CH), 128.13 (CH), 129.24 (C), 132.86 (βCH ΔAbu), 136.33 (C), 138.20 (C); 164.60 (C=O), 165.75 (C=O), 170.54 (C=O) ppm.

HRMS (ESI): calcd. for $C_{36}H_{38}N_4O_8$ 654.26896; found 655.27653 [M+1].

5.2.4. Synthesis of compound 14b:

To a stirred solution of trerephtaloyl chloride (50.75 mg, 0.25 mmol) in dry THF (5 mL), triethylamine (5.0 eq., 1.25 mmol, 0.18 mL) and H-(L)-Phe-*Z*-ΔPhe-OMe,TFA**, 8b,** (2.4 eq., 0.6 mmol, 262.8 mg) were successively added under nitrogen atmosphere. This mixture was stirred for 1 h at room temperature and then refluxed for 48 h under 80°C. The white precipitate was filtered and washed several times with abundant cold water to remove the byproduct Et_3NHCl and finally with ethyl ether. This white solid was dried under vacuum. Yield: 59%; mp: 240 – 243°C.

^{1}H-NMR (400 MHz, DMSO-d_6): δ = 3.031-3.092 (dd, 2H, J = 13.8 and 3.9 Hz, β-CH_2); 3.207-3.242 (dd, 2H, J = 13.8 and 10.8 Hz, β-CH_2); 3.703 (s, 6H, OCH_3); 4.862 (m, 2H, α-CH); 7.157-7.345 (m, 16H, H-Ar); 7.681 (m, 4H, H-Ar; ΔPhe); 7.278 (s, 3H, β-H; ΔPhe); 7.305-7.353 (m, 9H, H-Ar; ΔPhe); 7.875 (s, 4H, H-Ar, central ring); 8.844 (d, 2H, J = 8.0 Hz; αNH Phe); 9.963 (s, 2H, αNH ΔPhe).
^{13}C-NMR (100.6 MHz, DMSO): δ = 36.44 (βCH_2 Phe), 52.23 (OCH_3), 55.20 (αCH Phe), 125.93 (αC), 126.35 (CH), 127.37 (CH), 128.13 (CH), 128.57 (CH), 129.21 (CH), 129.52 (CH), 130.13 (CH), 132.04 (βCH ΔPhe), 133.25 (C), 136.26 (C), 138.27 (C), 165.36 (C=O), 165.86 (C=O), 171.46 (C=O) ppm.
HRMS (ESI): calcd. for $C_{46}H_{42}N_4O_8$ 778.30026; found 779.30759 [M+1]

5.2.5. Synthesis of compound 15:

5.2.5.1. Method 1:

This method uses the 2-2´-(1,3-phenylene) diacetic acid **21** and consisted in the synthesis of one amide linkage per each single step and the dehydration process only happens in the end of the synthetic route (Scheme 9).

5.2.5.1.1. Synthesis of 22:

The compound **21** (1.0 mmol, 0.1942 g) was dissolved in CH_2Cl_2 (10 mL) and the system was cooled in an ice bath. Next, DCC (1.1 eq., 2.2 mmol. 0.453 g) and NHS (1.1 eq., 2.2 mmol, 0.194 g) were added and the reaction was kept under stirring at room temperature for 3 hours. Then this suspension was filtered and the organic phase had its solvent evaporated. In another vial, the H-L-Phe-OH (1.1 eq., 2.2 mmol, 0.36 g) was dissolved in water (10 mL) and $NaHCO_3$ (2.3 eq. of the aa, 5 mmol, 0.34 mmol). The material, that was evaporated before, was dissolved in acetone (5 mL) and added to this aqueous reaction flask under vigorous stirring. The reaction was left reacting overnight and after the acetone was evaporated, the aqueous phase was acidified with aqueous HCl 1M until the pH got around 2. The reaction was filterd and resulted in a gel. An aliquote of this material was dissolved in ethyl acetate and the mixture was put in a separation funnel to exclude water from the material. The obtained organic phase was dried over anydrous $MgSO_4$ and evaporated. The final compound was isolated as an oil that after ^{1}H -NMR analyses revealed that the reaction was incomplete. So the rest of the filtred gel was dissolved in a mixture of dioxane (10 mL), water (10 mL) and aqueous NaOH 1M (2 mmol, 2 mL). This system was cooled in an ice bath, H-L-Phe-OH (1.1 eq., 2.2 mmol, 0.36 g) was added again and the pH was adjusted to 9 using aqueous NaOH 1M. The reaction was maintained under vigorous stirring at room temperature overnight. Next, the dioxane was evaporated and ethyl acetate (100 mL) was added to the reaction. The mixture was put in a separation funnel and aqueous $KHSO_4$ 1M was added until the pH reached 2. The organic phase was dried under anhydrous $MgSO_4$ and the solvent was evaporated under reduced pressure. This resulted in a pure white solid (87%, 0.424 g). mp. 145 – 146°C.

^{1}H-NMR (300 MHz, DMSO-d_6): 2.812-2.889 (dd, 2H, J = 13.8 and 9.3 Hz, CH_2; Phe), 3.013-3.075 (dd, 2H, J = 13.8 and 4.8 Hz, CH_2; Phe), 3.314 (d, 2H, J = 10.5Hz, CH_2), 3.368 (d, 2H, J = 10.5Hz, CH_2), 4.394-4.415 (m, 2H, αCH Phe), 6.930-7.270 (m, 14H, H-Ar), 8.339-8.366 (d, 2H, J = 8.1 Hz, N-H).

^{13}C-NMR (100.6 MHz, DMSO): δ= 36.777 (β CH_2 Phe), 41.822 ($\underline{C}H_2$), 53.538 (α CH Phe), 126.409 (CH), 126.863 (CH), 127.836 (CH), 128.171 (CH), 129.140 (CH), 129.899 (CH), 135.864 (C), 137.549 (C), 169.971 (C=O), 173.060 (C=O) ppm.

HRMS (ESI): calcd. for $C_{28}H_{28}N_2O_6$ 488.19474; found 511.18432 [M + Na^+].

5.2.5.1.2. Synthesis of 23:

The compound **22** (1.0 eq., 0.8 mmol, 0.39 g) was dissolved in acetonitrile (15 mL) and immersed in an ice bath. HOBt (2.0 eq., 1.6 mmol, 0.22 g), DCC (2.2 eq., 1.76 mmol, 0.364 g), H-DL-Phe(β-OH)-OMe (2.0 eq., 1.6 mmol, 2.84 g) and triethylamine (4.4 eq., 3.52 mmol, 0.5 mL) were added, waiting about 2 minutes between each addiction. The mixture was left stirring overnight. Next, the reaction was filtered to exclude the DCU and the liquid has been evaporated under reduced pressure. Then 60 mL of acetone was added and the flask was stored in the freezer for 3 hours to precipitate more DCU. So the reaction is filtered again and the liquid was evaporated. To the resulting yellow oil, 80 mL of ethyl acetate was added and this organic phase was washed successively with aqueous $KHSO_4$ 1M (3x 30 ml), $NaHCO_3$ 1M (3x 30 mL) and saturated NaCl (3x 30 ml) solutions. The organic phase was dried over anhydrous $MgSO_4$ and the solvent removed in vacuum. It resulted in a white solid that was recrystalized from dichloromethane/petroleum ether. The compound **6a** was obtained as a disteroisomeric mixture (44%, 0.30 g). This mixture was used with no purification in the next reaction step.

HRMS (ESI): calcd. for $C_{48}H_{50}N_4O_{10}$ 842.35269; found 843.35927 [M + 1].

5.2.5.1.3. Dehydration of 23:

The compound **23** (0.20 mmol, 0.165 g) was dissolved in 7 mL of dry acetonitrile. DMAP (0.11 eq.0.04 mmol, 6 mg) and Boc_2O (1.1 eq., 0.4 mmol, 0.105 g) were added under stirring at room temperature. The reaction has been followed by ^1H -NMR and after proving that the initial material was all consumed, TMG (0,02 mL/mL of solvent; 0,14 mL) was joined to the reaction. After 24 hours there was evidence, by ^1H –NMR, that all the material was converted into the desirable product, **15,** which precipitated in the reaction media. So the reaction was filtrated and 59 mg of a solid was collected. The organic liquid phase was evaporated and the resulting oil was dissolved in CH_2Cl_2 (50 ml) and this material was washed successively with aqueous $KHSO_4$ 1M (2x 30 ml), and saturated NaCl (1x 50 ml) solutions. The organic phase was dried over anhydrous

$MgSO_4$ and the solvent removed in vacuum. It was obtained an oil that was crystalized from CH_2Cl_2/ petroleum ether. A white solid (99 mg; 62%) was obtained.

^{1}H-NMR (300 MHz, DMSO-d_6): 2.784-2.843 (dd, 2 H, J = 13.6 and 10.0 Hz, β CH_2 Phe), 3.088-3.133 (dd, 2 H, J = 13.6 and 4.0 Hz, β CH_2 Phe), 3.283 (d, 2H, J = 13.8 Hz, CH2), 3.353 (d, 2H, J = 13.8 Hz, CH2), 3.684 (s, 6 H, OCH_3), 4.649-4.703 (m, 2 H, α CH), 6.860-6.879 (d, 2 H, J = 7.6 Hz, H-Ar; central ring), 6.891 (s, 1 H, H-Ar, central ring), 6.995-7.032 (t, 1H, J = 7.6 Hz, H-Ar; central ring), 7.279 (s, 2 H, β H ΔPhe), 7.167-7.333 (m, 16 H, H-Ar, Phe + ΔPhe), 7.587-7.609 (m, 4 H, H-Ar, o-ΔPhe), 8.415-8.435 (d, 2 H, J = 8.0 Hz, αNH Phe), 9.896 (s, 2H, αNH ΔPhe).

^{13}C-NMR (100.6 MHz, DMSO): δ = 37.14 (βCH_2 Phe), 41.88 (CH2), 52.17 (OCH_3), 54.09 (αCH Phe), 126.31 (CH), 126.75 (CH), 127.77 (CH), 128.07 (CH), 128.55 (CH), 129.22 (CH), 129.40 (CH), 129.96 (CH), 130.03 (CH), 131.90 (βCH ΔPhe), 125.98 (C), 133.24 (C), 135.86 (C), 137.76 (C), 165.40 (C=O), 170.04 (C=O), 171.46 (C=O) ppm.
HRMS (ESI): calcd. for $C_{48}H_{46}N_4O_8$ 806.33156; found 807.33796 [M+1].

5.2.5.2.Method 2:

In a 50-mL round-bottom flask equipped with a stir bar and a condenser, containing 2-2′-(1,3-phenylene)diacetic acid (0.097 g, 0.50 mmol) **21** thionyl chloride (117.03 mmol, 8.5 mL) was added with an addition funnel. Then four drops of DMF was gathered and the reaction was kept under a 60 °C reflux for 6 hours. Then the excess of thionyl chloride was evaporated and the resulting residue was dissolved in dry THF (5 mL). Next, triethylamine (5.0 eq., 2.5 mmol, 0.35 mL) and H-L-Phe-*Z*-ΔPhe-OMe,TFA**, 8b,** (2.4 eq., 1.2 mmol, 525.6 mg) were added under nitrogen atmosphere. This mixture was stirred for 1 h at room temperature and then refluxed for 48 h under 80°C. The white precipitate was filtered and washed several times with abundant cold water to remove the byproduct Et_3NHCl and finally with ethylic ether. This white solid was dried under vacuum. Yield: 47%.

5.2.6. Synthesis of compound 16a:

To a stirred solution of diphenyl acetyl chloride (97.5 mg, 0.43 mmol) in dry THF (5 mL), triethylamine (2.5 eq., 1.07 mmol, 0.15 mL) and then H-L-Phe-*Z*-ΔAbu-OMe,TFA**, 8b,** (1.1 eq., 0.47 mmol, 175 mg) were added under nitrogen atmosphere. This mixture was stirred for 48h at room temperature and then the reaction was filtered, the solid was, separated, washed with water, to remove Et_3NHCl, and successively washed with aqueous $KHSO_4$ 1M (10 mL), $NaHCO_3$ 1M (10 mL) and Brine (10 mL) and ethyl ether. The filtered organic THF phase was evaporated and 20 mL of ethyl acetate was added to the resultant material and the suspension was stored in the freezer for 24h. The suspension was filtered and the solid was washed again following the same procedure as had been done before. All the solids were pure and corresponded to the compound **13a** that was obtained as a white solid. Yield: 82%; mp: 173 – 175°C.

^{1}H-NMR (400 MHz, DMSO-d_6): δ = 1.555-1.573 (d, 3 H, *J* = 7.2 Hz, γCH_3 ΔAbu), 2.791-2.849 (dd, 1 H, *J* = 13.6 and 9.6 Hz, βCH_2), 3.034-3.081 (dd, 3 H, *J* = 4.8 and 13.6 Hz, βCH_2 Phe), 3.593 (s, 3 H, OCH_3), 4.711-4.769 (m, 1 H, αCH Phe), 5.029 (s, 1H, H-C(Phe)$_2$) 6.501 (q, 1 H, *J* = 7.2 Hz, βCH ΔAbu), 6.973-6.996 (dd, 2H, J=7.2 and 1.6 Hz, H-mAr, Phe), 7.154-7.264 (m, 13 H, H-Ar), 8.609 (d, 1H, J = 8.4 Hz, αNH Phe), 9.493 (s, 3 H, αNH ΔAbu) ppm.

^{13}C-NMR (100.6 MHz, DMSO): δ = 13.35 (γCH_3 ΔAbu), 37.83 (βCH_2 Phe), 51.81 (OCH_3), 53.76 (αCH Phe), 56.00 (C-(Phe)$_2$), 127.59 (αC), 126.39 (CH), 128.01 (CH), 128.11 (CH), 128.40 (CH), 128.70 (CH), 129.27 (CH), 132.47(βCH ΔAbu), 137.43 (C), 140.07(C), 140.30 (C), 164.54 (C=O), 170.24 (C=O), 170.79 (C=O) ppm.

HRMS (ESI): calcd. for $C_{28}H_{28}N_2O_4$ 456.20491; found 457.21191 [M + 1].

5.2.7. Synthesis of compound 16b:

To a stirred solution of diphenyl acetyl chloride (57.5 mg, 0.25 mmol) in dry THF (5 mL) was added triethylamine (2.5 eq., 0.63 mmol, 0.10 mL) and then H-L-Phe-*Z*-ΔPhe-OMe,TFA**, 8b,** (1.1 eq., 0.28 mmol, 120.5 mg) was added under nitrogen

atmosphere. This mixture was stirred for 48 h at room temperature and then the white precipitate was filtered and washed several times with water to remove the byproduct Et_3NHCl and finally with aqueous $KHSO_4$ 1M (10 mL), $NaHCO_3$ 1M (10 mL) and Brine (10 mL) and eyhyl ether. The filtered THF phase was taken apart and diethyl ether was added and the dispersion was stored into the freezer for 24 h to precipitate more product. This new solid was filtered and washed the same way as before. Both solids were pure and corresponded to the desired product **16b**. Yield: 71%; 197 – 198°C.

^{1}H-NMR (400 MHz, DMSO-d_6): δ = 2.778-2.838 (dd, 1H, J= 13.8 and 10.2 Hz, βCH_2); 3.073-3.118 (dd, 1H, J = 13.8 and 4.4 Hz, βCH_2); 3.647 (s, 3H, OCH_3); 4.746-4.781 (m, 1H, α-CH); 5.002 (s, 1H, H-C(Phe)2); 6.953-6.977 (m, 2H, Phe), 7.144-7.312 (m, 17H, H-Ar + βH ΔPhe), 7.554-7.572 (d, 2H, J = 7.2 Hz, H-oAr; ΔPhe), 8.638 (d, 1H, J = 8.4 Hz, αNH Phe), 9.951 (s, 1 H, αNH ΔPhe) ppm.

^{13}C-NMR (100.6 MHz, DMSO): δ = 37.41 (βCH_2 Phe), 52.35 (OCH_3), 54.10 (αCH Phe), 56.14 (C-$(Phe)_2$), 125.81 (αC), 126.49 (CH), 128.18 (CH), 128.20 (CH), 128.44 (CH), 128.71 (CH), 128.87 (CH), 129.36 (CH), 130.14 (CH), 132.33 (βCH ΔPhe), 133.23 (C), 137.62 (C), 140.11(C), 140.48 (C), 165.50 (C=O), 171.12 (C=O), 171.44 (C=O) ppm.

HRMS (ESI): calcd. for $C_{33}H_{30}N_2O_4$ 518.22056; found 519.22815 [M + 1].

5.2.8. Synthesis of compound 24

5.2.8.1. Acetylation of the caffeic acid (CA):

In a 50-mL round-bottom flask, caffeic acid (5.5 mmol, 1 g) was dissolved in a solution of NaOH 1M (15 mL) with magnetic stirring. To this solution, acetic anhydride (2 mL, 2.164 g, 21.2 mmol) was added. The reaction mixture was stirred for 30 minutes in an ice bath. The impure solid product was isolated using vacuum filtration. The solid was washed with a minimal amount of ice-cold distilled water. The crude product was recrystalized by dissolving it in 15 mL of boiling ethanol (95%). The solution rested to allow the solution to cool slowly to room temperature, and let the crystals form for half

an hour. The pure product was isolated using vacuum filtration after cooling in an ice bath for 10 minutes. The product was left resting in an open vial for half an hour, in order to dry. 1.27 g of a white solid was obtained with 87% yield. mp 190-192 ^{o}C.

^{1}H-NMR (DMSO-d$_6$): δ = 7.7 (br s, 1H, Har), 7.55 (d, 1H, J = 18.6 Hz, CHCar), 7.2 (d, 2H, J = 8.6 Hz, Har), 6.5 (d, 1H, J = 18.6 Hz, CHCO), 2.3 (s, 6H, 2 x OAc);

^{13}C-NMR (DMSO-d$_6$): δ = 168.2, 168.1, 167.4, 143.3, 142.3, 142.2, 133.1, 126.7, 124.1, 123.0, 120.3, 20.4, 20.3; LRMS: 265.1, 205.1, 163.1, 145.1, 117.1, 89.1;

HRMS: calc. for $C_{13}H_{12}O_6$ + (Na+): 287.0526; found: 287.0522.

5.2.8.2. Coupling of the diacetylated caffeic acyl chloride to the dehydropeptide 8b

4 mL of thionyI chloride was slowly added to a 10-mL round-bottom flask equipped with a stir bar and condenser, containing the diacetylcaffeic acid (0.47 mmol, 125 mg). Then two drops of DMF was gathered to the reaction media and the reaction was kept in a 60°C reflux for 4 hours. Then the excess of thionyl chloride was evaporated and the resulting residue was dissolved in dry THF (5 mL). Next, triethylamine (1.25 eq., 1.19 mmol, 0.17 mL) and H-L-Phe-*Z*-ΔPhe-OMe,TFA**, 8b,** (1.1 eq., 0.52 mmol, 226.5 mg) were added under nitrogen atmosphere. This mixture was stirred for 1 h at room temperature and then refluxed for 24 h under 80°C. Then the reaction was filtered to eliminate the triethylamonium chloride. The THF was evaporated and the residue was dissolved in 100 mL of CH_2Cl_2. This solution was washed successively with aqueous $KHSO_4$ 1M (4x 30 mL), $NaHCO_3$ 1M (1x 30 mL) and Brine (3x 30 mL). The organic phase was dried over anhydrous $MgSO_4$, filtered and evaporated under reduced pressure. It was obtained an oil that crystallized in ethyl acetate/diethylic ether. After filtration of the precipitate, it resulted in the product **24** as an orange solid (142 mg, 52%).

^{1}H-NMR (DMSO-d$_6$): δ = 2.273 (s, 3H, CH_3-Ac), 2.280 (s, 3H, CH_3-Ac), 2.829-2.889 (dd, 1H, *J* = 13.9, 10.2 Hz, β CH_2), 3.140-3.186 (dd, *J* = 13.9, 4.3 Hz, 1H), 3.701 (s, 3H, OCH_3), 4.794-4.816 (ddd, *J* = 10.2, 8.2, 4.3 Hz, 1H, αCH), 6.670 (d, 1H, *J* = 15.8 Hz, =CH), 7.173 – 7.215 (m, 1H, H-Ar), 7.255 (br s, 1H, βH ΔPhe), 7.279-7.402 (m, 9H, =CH + H-Ar), 7.496 – 7.460 (m, 2H, H-Ar), 7.628 – 7.652 (m, 2H, H-Ar), 8.483 (d, 1H, *J* = 8.4 Hz, αNH Phe), 9.940(s, 1H, αNH ΔPhe).

^{13}C-NMR (100.6 MHz, DMSO): δ = 20.37 (CH_3 Ac), 37.10 (βCH_2 Phe), 52.24 (OCH_3), 54.39 (αCH Phe), 125.92 (αC), 122.33 (CH), 122.82 (CH), 124.18 (CH), 125.94 (CH), 126.44 (CH), 128.18 (CH), 128.62 (CH), 129.21 (CH), 129.52 (CH), 130.13 (CH), 137.48 (CH), 132.05 (βCH ΔPhe), 133.22 (C), 133.69 (C), 137.80(C), 142.32 (C), 142.76 (C), 164.77 (C=O), 165.35 (C=O), 168.19 (C=O), 168.23 (C=O), 171.43 (C=O) ppm.

HRMS (ESI): calcd. for $C_{32}H_{30}N_2O_8$ 570.20022; found 571.20805 [M + 1].

5.2.9. Synthesis of compound 26

5.2.9.1. Acetylation of the dihydrocaffeic acid (DHCA):

In a 50-mL round-bottom flask, dihydrocaffeic acid (5.5 mmol, 1 g) was dissolved in a solution of NaOH 1M (15 mL) under magnetic stirring. To this solution, acetic anhydride was added. The reaction mixture was stirred for 2 hours in an ice bath. An oil was formed in the bottom of the reaction flask. The aqueous media was removed with a Pasteur pipette and the excess of solvent was removed from the oil by evaporation under reduced pressure. In the end, an slightly yellow oil was obtained (1.05 g, 72%).

^{1}H-NMR (300 MHz, DMSO-d_6): δ = 2.233 (s, 3H, OAc), 2.240 (s, 3H, OAc), 2.342 (t, 3H, J = 8.1 Hz, CH_2), 2.775 (t, 3H, J = 8.1 Hz, CH_2), 7.107-7.073 (m, 3H, Har).

5.2.9.2. Coupling of the diacetylated dihydrocaffeic acyl chloride to the dehydropeptide 8b:

4 mL of thionyI chloride was slowly added to a 10-mL round-bottom flask equipped with a stir bar and condenser, containing the diacetyldihydrocaffeic acid (0.47 mmol, 125 mg). Then two drops of DMF was gathered to the reaction media and the reaction was kept under a 60°C reflux for 4 hours. Then the excess of thionyl chloride was evaporated and the resulting residue was dissolved in dry THF (5 mL). Next, triethylamine (1.25 eq., 1.19 mmol, 0.17 mL) and H-L-Phe-*Z*-ΔPhe-OMe,TFA**, 8b,** (1.1 eq., 0.52 mmol, 226.5 mg) were added under nitrogen atmosphere. This

mixture was stirred for 1 h at room temperature and then refluxed for 24 h under 80°C. Then the reaction was filtered to eliminate the triethylamonium chloride. The THF was evaporated and the residue was dissolved in 100 mL of CH_2Cl_2. This solution was washed successively with aqueous $KHSO_4$ 1M (4x 30 mL), $NaHCO_3$ 1M (1x 30 mL) and Brine (3x 30 mL). The organic phase was dried over anhydrous $MgSO_4$, filtered and evaporated under reduced pressure. It was obtained an oil that crystallized in ethyl acetate/diethyl ether. After filtration of the precipitate, it resulted in the product **26** as an orange solid (176 mg; 64%).

^{1}H-NMR (400 Hz, DMSO-d_6): δ = 2.228 (s, 3H, CH_3-Ac), 2.231 (s, 3H, CH_3-Ac), 2.371 (t, J = 7.9 Hz, 2H, CH_2), 2.704 (t, J = 7.9 Hz, 2H, CH_2), 2.829-2.889 (dd, 1H, *J* = 13.8, 10.2 Hz, β CH_2), 3.085-3.130 (dd, *J* = 13.8, 4.4 Hz, 1H), 3.688 (s, 3H, OCH_3), 4.652-4.709 (m, 1H, αCH), 7.004 – 7.057 (m, 2H, H-Ar), 7.189-7.207 (m, 2H, H-Ar), 7.247 (s, 1 H, βH ΔPhe), 7.265-7.362 (m, 7 H, H-Ar), 8.357 (d, 1H, *J* = 8.4 Hz, αNH Phe), 9.922 (s, 1H, αNH ΔPhe).

^{13}C-NMR (100.6 MHz, DMSO): *δ* = 20.31 (CH_3 Ac), 20.33 (CH_3 Ac), 30.24 (CH2), 36.45 (CH2), 37.08 (βCH_2 Phe), 52.16 (OCH_3), 54.10 (αCH Phe), 125.96 (αC), 123.06 (CH), 123.19 (CH), 126.13 (CH), 126.30 (CH), 128.04 (CH), 128.53 (CH), 129.21 (CH), 129.45 (CH), 130.08 (CH), 131.99 (βCH ΔPhe), 133.20 (C), 137.91 (C), 140.01(C), 140.08 (C), 141.65 (C), 165.35 (C=O), 168.16 (C=O), 168.27 (C=O), 171.30 (C=O), 171.58 (C=O) ppm.

HRMS (ESI): calcd. for $C_{32}H_{32}N_2O_8$ 572.21587; found 595.20453 [M + Na^+].

5.3. Basic hydrolysis of the methyl esters

The general procedure for the hydrolysis of the methyl esters groups was to dissolve the proper amount of each compound into a mixture of dioxane (3 mL/0.1 mmol of the ester) and aqueous NaOH 1M (1.5 eq. / each ester group) under vigorous stirring and at room temperature. This process was followed by t.l.c. (eluent: ethyl acetate). When all the initial reactant was consumed, the solvent was evaporated and 10 mL of $KHSO_4$ 1M was added to the reaction vial to assure that the pH reached values around 2-3. This system was kept at the freezer for 24 h and then the product was filtered, washed with aqueous $KHSO_4$ 1M and with a minimum amount of diethyl ether. The solid obtained was dried under vacuum.

5.3.1. Synthesis of compound 17a:

The general procedure described above was followed using compound **13a** (0.075 mmol, 80 mg), giving compound **17a** (82 %) as a white solid, that decomposes at 197°C.

^{1}H-NMR (400 MHz, DMSO-d_6): δ = 1.613-1.631 (d, 9 H, *J* = 7.2 Hz, γCH_3 ΔAbu), 3.003-3.064 (dd, 3 H, *J* = 13.6 and 10.8 Hz, βCH_2), 3.171-3.205 (dd, 3 H, *J* = 3.6 and 13.6 Hz, βCH_2 Phe), 4.888-4.946 (m, 3 H, αCH Phe), 6.571-6.589 (q, 3 H, *J* = 7.2 Hz, βCH ΔAbu), 7.130-7.166 (m, 6 H, H-mAr), 7.217-7.276 (t, 3H, J = 7.6 Hz, H-pAr), 7.357-7.375 (d, 6 H, J = 7.2 Hz, H-oAr), 8.293 (s, 3H, H-Ar; central ring), 8.804-8.825 (d, 3H, J = 8.4 Hz, αNH Phe), 9.373 (s, 3 H, αNH ΔAbu) ppm.

^{13}C-NMR (100.6 MHz, DMSO): δ = 13.72 (γCH_3 ΔAbu), 39.34 (βCH_2 Phe), 54.93 (αCH Phe), 128.14 (αC), 126.30 (CH), 128.11 (CH), 129.14 (2CH)*, 129.19, 132.43 (βCH ΔAbu), 134.32 (C), 138.09 (C); 165.45 (C=O), 165.47 (C=O), 170.10 (C=O) ppm.

HRMS (ESI): calcd. for $C_{48}H_{48}N_6O_{12}$ 900.33302; found 901.33976 [M + 1].

5.3.2. Synthesis of compound 17b:

The general procedure described above was followed using compound **13b** (0.053 mmol, 60 mg) giving compound **17b** (85 %, 49 mg) as a white solid, that decomposes at 224°C.

^{1}H-NMR (400 MHz, DMSO-d_6): δ = 3.016-3.078 (dd, 3H, J = 13.9 and 10.8 Hz, βCH_2); 3.016-3.078 (dd, 3H, J=13.9 and 4.0 Hz, βCH_2); 4.886-4.943 (m, 3H, αCH); 7.131-7.202 (t, 3H, J = 7.2 Hz); 7.220-7.354 (m, 15H, H-Ar); 7.298 (s, 3H, β-H; ΔPhe); 7.386-7.404 (m, 6H, H-Ar); 7.638-7.659 (m, 6H, H-Ar; ΔPhe); 8.341 (s, 3H, H-Ar; central ring); 8.899-8.920 (d, 3H, J = 8.4 Hz; αNH Phe); 9.819 (s, 3H, αNH ΔPhe).

^{13}C-NMR (100.6 MHz, DMSO): *δ* = 33.33 (βCH_2 Phe), 55.16 (αCH Phe), 126.65 (αC), 126.29 (CH), 128.17 (CH), 128.48 (CH), 129.17 (2 CH), 129.23 (CH), 129.94 (CH), 131.84 (βCH ΔPhe), 133.56 (C), 134.35 (C), 138.22 (C), 165.71 (C=O), 166.18 (C=O), 171.08 (C=O) ppm.

HRMS (ESI): calcd. for $C_{63}H_{54}N_6O_{12}$ 1086.37997; found 1087.38470 [M + 1].

5.3.3. Synthesis of compound 18a:

The general procedure described above was followed using compound **14a** (0.153 mmol, 100 mg) giving compound **18a** (68 %, 43 mg) as a white solid, that decomposes at 190°C.

^{1}H-NMR (400 MHz, DMSO-d_6): δ = 1.626-1.644 (d, 6 H, *J* = 7.2 Hz, γCH_3 ΔAbu), 3.994-3.056 (dd, 2 H, *J* = 13.6 and 10.0 Hz, βCH_2), 3.157-3.201 (dd, 2 H, *J* = 4.0 and 13.6 Hz, βCH_2 Phe), 4.827-4.886 (m, 2 H, αCH Phe), 6.575-6.593 (q, 2 H, *J* = 7.2 Hz, βCH ΔAbu), 7.226-7.264 (t, 3H, J = 7.6 Hz, H-pAr), 7.375-7.394 (d, 4 H, J = 7.2 Hz, H-oAr), 7.129-7.166 (m, 4 H, H-mAr), 7.814 (s, 4H, H-Ar; central ring), 8.706-8.727 (d, 2H, J = 8.4 Hz, αNH Phe), 9.353 (s, 2 H, αNH ΔAbu) ppm.

^{13}C-NMR (100.6 MHz, DMSO): δ = 13.73 (γCH_3 ΔAbu), 37.28 (βCH_2 Phe), 54.94 (αCH Phe), 128.19 (αC), 126.28 (CH), 127.28 (CH), 128.06 (CH), 129.22 (C), 132.37 (βCH ΔAbu), 136.33 (C), 138.27 (C); 165.49 (C=O), 165.66 (C=O), 170.17 (C=O) ppm.

HRMS (ESI): calcd. for $C_{34}H_{34}N_4O_8$ 626.23766; found 627.24519 [M + 1].

5.3.4. Synthesis of compound 18b:

The general procedure described above was followed using compound **14b** (0.077 mmol, 60 mg) giving compound **18b** (78%, 45 mg) as a white solid, that decomposes at 218°C.

^{1}H-NMR (400 MHz, DMSO-d_6): δ =.3.015-3.077 (dd, 2H, J = 13.7 and 10.8 Hz, βCH_2); 3.207-3.242 (dd, 2H, J = 13.7 and 3.6, βCH_2); 4.838-4.886 (m, 2H, αCH); 7.143-7.334 (m, 14H, H-Ar + βCH ΔPhe); 7.400-7.418 (d, 4H, J = 7.2 Hz, H-Ar; Phe); 7.651-7.669 (m, 4H, H-Ar; ΔPhe); 7.854-7.865 (m, 4H, H-Ar, central ring); 8.786-8.807 (d, 2H, J = 8.4 Hz; αNH Phe); 9.789 (s, 2H, αNH ΔPhe).

^{13}C-NMR (100.6 MHz, DMSO): *δ* = 36.52 (βCH_2 Phe), 55.24 (αCH Phe), 126.60 (αC), 126.30 (CH), 127.33 (CH), 128.09 (CH), 128.47 (CH), 129.21 (CH), 129.24 (CH), 130.02 (CH), 131.87 (βCH ΔPhe), 133.60 (C), 136.28 (C), 138.36 (C), 165.80 (C=O), 166.20 (C=O), 171.12 (C=O) ppm.

HRMS (ESI): calcd. for $C_{44}H_{38}N_4O_8$ 750.26896; found 751.27670 [M + 1].

5.3.5. Synthesis of compound 19:

The general procedure described above was followed using compound **15** (0.081 mmol, 65 mg) giving compound **19** (64%, 40 mg) as a white solid, that decomposes at 198°C.

^{1}H-NMR (300 MHz, DMSO-d_6): 2.759-2.820 (dd, 2 H, J = 13.8 and 10.6 Hz, β CH_2 Phe), 3.100-3.144 (dd, 2 H, J = 13.8 and 3.8 Hz, β CH_2 Phe), 3.283 (d, 2H, J =13.8 Hz, CH2), 3.353 (d, 2H, J = 13.8 Hz, CH2), 4.653-4.709 (m, 2 H, α CH), 6.822-6.841 (m, 3 H, H-Ar; central ring), 6.968-7.006 (t, 1H, J = 8 Hz, H-Ar; central ring), 7.280 (s, 2 H, β H ΔPhe), 7.156-7.323 (m, 16 H, H-Ar, Phe + ΔPhe), 7.586-7.601 (m, 4 H, H-Ar, o-ΔPhe), 8.354-8.375 (d, 2 H, J = 8.4 Hz, αNH Phe), 9.713 (s, 2H, αNH ΔPhe).

^{13}C-NMR (100.6 MHz, DMSO): δ = 37.14 (βCH_2 Phe), 41.88 (CH2), 54.07 (αCH Phe), 126.26 (CH), 126.70 (CH), 127.73 (CH), 128.02 (CH), 128.11 (CH), 128.45 (CH), 129.18 (CH), 129.22 (CH), 129.92 (CH), 131.80 (βCH ΔPhe), 126.56 (C), 133.54 (C), 135.82 (C), 137.82 (C), 166.18 (C=O), 170.00 (C=O), 171.13 (C=O) ppm.

HRMS (ESI): calcd. for $C_{46}H_{42}N_4O_8$ 778.30026; found 779.30758 [M + 1].

5.3.6. Synthesis of compound 20a:

The general procedure described above was followed using compound **16a** (0.30 mmol, 136 mg) giving compound **20a** (71%, 91.2 mg) as a white solid, that decomposes at 190°C.

^{1}H-NMR (400 MHz, DMSO-d_6): δ = 1.536-1.553 (d, 3 H, *J* = 6.8 Hz, γCH_3 ΔAbu), 2.775-2.834 (dd, 2 H, J = 14.0 and 9.8 Hz, β CH_2 Phe), 3.044-3.090 (dd, 2 H, J = 14.0 and 4.5 Hz, β CH_2 Phe), 4.76 (ddd, 1 H, *J* = 9.8, 8.4, 4.5 Hz, α CH Phe), 5.016 (s, 1H, H-C(Phe)$_2$) 6.516-6.569 (q, 1 H, *J* = 7.2 Hz, βCH ΔAbu), 6.955-6.979 (m, 2H, H-mAr, Phe), 7.152-7.283 (m, 13H, H-Ar), 8.501-8.522 (d, 1H, J = 8.4 Hz, αNH Phe), 9.298 (s, 3 H, αNH ΔAbu) ppm.

^{13}C-NMR (100.6 MHz, DMSO): δ = 13.61 (γCH_3 ΔAbu), 37.92 (βCH_2 Phe), 53.75 (αCH Phe), 56.02 (C-(Phe)$_2$), 128.01 (αC), 126.21 (CH), 126.35 (CH), 126.55 (CH), 127.97 (CH), 127.98 (CH), 128.11 (CH), 128.40 (CH), 128.70 (CH), 129.28 (CH),

132.22 (βCH ΔAbu), 137.50 (C), 140.05 (C), 140.30 (C), 165.42 (C=O), 169.85 (C=O), 170.77 (C=O) ppm.

HRMS (ESI): calcd. for $C_{27}H_{26}N_2O_4$ 442.18926; found 443.19717 [M + 1].

5.3.7. Synthesis of compound 20b:

The general procedure described above was followed using compound **16b** (0.108 mmol, 50 mg) giving compound **20b** (73%, 35 mg) as a white solid, that decomposes at 197°C.

^{1}H-NMR (400 MHz, DMSO-d_6): δ = 2.778-2.838 (dd, 1H, J = 13.8 and 10.8 Hz, βCH_2); 3.073-3.118 (dd, 1H, J = 13.8 and 4.0 Hz, βCH_2); 4.755-4.812 (m, 1H, α-CH); 4.995 (s, 1H, H-C(Phe)$_2$); 6.932-6.952 (m, 2H, Phe), 7.148-7.299 (m, 17 H, H-Ar + βH ΔPhe), 7.554-7.572 (dd, 2H, J = 7.2 and 1.2 Hz, H-oAr; ΔPhe), 8.569-8.590 (d, 1H, J = 8.4 Hz, αNH Phe), 9.773 (s, 1 H, αNH ΔPhe) ppm.

^{13}C-NMR (100.6 MHz, DMSO): δ = 37.28 (βCH_2 Phe), 53.93 (αCH Phe), 56.00 (C-(Phe)$_2$), 126.35 (αC), 126.32 (CH), 127.97 (CH), 128.10 (CH), 128.30 (CH), 128.43 (CH), 128.75 (CH), 129.24 (CH), 129.88 (CH), 131.94 (βCH ΔPhe), 133.52 (C), 137.61 (C), 140.00 (C), 140.40 (C), 166.16 (C=O), 170.87 (C=O), 170.92 (C=O) ppm

HRMS (ESI): calcd. for $C_{32}H_{28}N_2O_4$ 504.20491; found 505.21252 [M + 1].

6. Bibliography

1. de Loos, M.; Feringa, B. L.; van Esch, J. H. *Eur.J.Org.Chem.* **2005**, *2005*, 3615-3631.
2. Mitra, R. N.; Das, D.; Roy, S.; Das, P. K. *Journal of Physical Chemistry B* **2007**, *111*, 14107-14113.
3. Hamidi, M.; Azadi, A.; Rafiei, P. *Advanced Drug Delivery Reviews* **2008**, *60*, 1638-1649.
4. Almdal, K.; Dyre, J.; Hvidt, S.; Kramer, O. *Polymer Gels and Networks* **1993**, *1*, 5-17.
5. Peppas, N. A.; Khare, A. R. *Advanced Drug Delivery Reviews* **1993**, *11*, 1-35.
6. M. Hamidi, A. Azadi, P. Rafiei. Advanced Drug Delivery Reviews 60 (2008) 1638–1649.
7. Peppas, N. A.; Bures, P.; Leobandung, W.; Ichikawa, H. *European Journal of Pharmaceutics and Biopharmaceutics* **2000**, *50*, 27-46.
8. Satish, C. S.; Kumar, C.; Narasimhamurthy, S.; Shivakumar, H. G. *Indian Journal of Pharmaceutical Education and Research* **2007**, *41*, 195-204.
9. Ryan, D. M.; Nilsson, B. L. *Polymer Chemistry* **2012**, *3*, 18-33.
10. Hennink, W. E.; van Nostrum, C. F. *Advanced Drug Delivery Reviews* **2002**, *54*, 13-36.
11. Blanco, M. D.; Garcia, O.; Trigo, R. M.; Teijon, J. M.; Katime, I. *Biomaterials* **1996**, *17*, 1061-1067.
12. Tibbitt, M. W.; Anseth, K. S. *Biotechnology and Bioengineering* **2009**, *103*, 655-663.
13. Lakshmanan, A.; Hauser, C. A. E. *International Journal of Molecular Sciences* **2011**, *12*, 5736-5746.
14. Fung, S. Y.; Keyes, C.; Duhamel, J.; Chen, P. *Biophysical Journal* **2003**, *85*, 537-548.
15. Truong, W. T.; Su, Y. Y.; Meijer, J. T.; Thordarson, P.; Braet, F. *Chemistry-An Asian Journal* **2011**, *6*, 30-42.
16. Chen, C. S.; Mrksich, M.; Huang, S.; Whitesides, G. M.; Ingber, D. E. *Science* **1997**, *276*, 1425-1428.
17. Discher, D. E.; Janmey, P.; Wang, Y. L. *Science* **2005**, *310*, 1139-1143.
18. Qiu, Y.; Park, K. *Advanced Drug Delivery Reviews* **2001**, *53*, 321-339.
19. Yang, Z. M.; Liang, G. L.; Ma, M. L.; Gao, Y.; Xu, B. *Journal of Materials Chemistry* **2007**, *17*, 850-854.
20. Lehn, J. M. *Proceedings of the National Academy of Sciences of the United States of America* **2002**, *99*, 4763-4768.
21. Yan, X. H.; Zhu, P. L.; Li, J. B. *Chemical Society Reviews* **2010**, *39*, 1877-1890.
22. van Esch, J. H. *Langmuir* **2009**, *25*, 8392-8394.
23. Yang, Z.; Liang, G.; Xu, B. *Accounts of Chemical Research* **2008**, *41*, 315-326.
24. Jayawarna, V.; Ali, M.; Jowitt, T. A.; Miller, A. E.; Saiani, A.; Gough, J. E.; Ulijn, R. V. *Advanced Materials* **2006**, *18*, 611-+.
25. Wang, H. M.; Ren, C. H.; Song, Z. J.; Wang, L.; Chen, X. M.; Yang, Z. M. *Nanotechnology* **2010**, *21*.
26. Sangeetha, N. M.; Maitra, U. *Chem.Soc.Rev.* **2005**, *34*, 821-836.
27. Loo, Y.; Zhang, S. G.; Hauser, C. A. E. *Biotechnology Advances* **2012**, *30*, 593-603.

28. (a) Ulijn, R. V.; Smith, A. M. *Chemical Society Reviews* **2008**, *37*, 664-675; (b) Cavalli S., Albericio F., Kros A. *Chem.Soc.Rev*., 2010, 39, 241–263.
29. Madhavaiah, C.; Verma, S. *Chemical Communications* **2004**, 638-639.
30. Matsumura, S.; Uemura, S.; Mihara, H. *Chemistry-A European Journal* **2004**, *10*, 2789-2794.
31. Aggeli, A.; Bell, M.; Boden, N.; Keen, J. N.; Knowles, P. F.; Mcleish, T. C. B.; Pitkeathly, M.; Radford, S. E. *Nature* **1997**, *386*, 259-262.
32. Zhao, X. J.; Zhang, S. G. *Trends in Biotechnology* **2004**, *22*, 470-476.
33. Matsuura, K.; Murasato, K.; Kimizuka, N. *Journal of the American Chemical Society* **2005**, *127*, 10148-10149.
34. a) Khazanovich, N.; Granja, J. R.; McRee, D. E.; Milligan, R. A.; Ghadiri, M. R. *J.Am.Chem.Soc.* **1994**, *116*, 6011-6012; b) Bong, D. T.; Clark, T. D.; Granja, J. R.; Ghadiri, M. R. *Angewandte Chemie International Edition* **2001**, *40*, 988-1011.
35. Hartgerink, J. D.; Beniash, E.; Stupp, S. I. *Proceedings of the National Academy of Sciences of the United States of America* **2002**, *99*, 5133-5138.
36. Santoso, S.; Hwang, W.; Hartman, H.; Zhang, S. G. *Nano Letters* **2002**, *2*, 687-691.
37. Yokoi, H.; Kinoshita, T.; Zhang, S. G. *Proceedings of the National Academy of Sciences of the United States of America* **2005**, *102*, 8414-8419.
38. Kar, T.; Mandal, S. K.; Das, P. K. *Chemistry-A European Journal* **2011**, *17*, 14952-14961.
39. Reches, M.; Gazit, E. *Science* **2003**, *300*, 625-627.
40. Zhang, Y.; Gu, H. W.; Yang, Z. M.; Xu, B. *Journal of the American Chemical Society* **2003**, *125*, 13680-13681.
41. Chen, L.; Morris, K.; Laybourn, A.; Elias, D.; Hicks, M. R.; Rodger, A.; Serpell, L.; Adams, D. J. *Langmuir* **2010**, *26*, 5232-5242.
42. Reches, M.; Gazit, E. *Isr.J.Chem.* **2005**, *45*, 363-371.
43. Johnson, E. K.; Adams, D. J.; Cameron, P. J. *Journal of Materials Chemistry* **2011**, *21*, 2024-2027.
44. Zhang, Y.; Yang, Z. M.; Yuan, F.; Gu, H. W.; Gao, P.; Xu, B. *Journal of the American Chemical Society* **2004**, *126*, 15028-15029.
45. Yang, Z. M.; Gu, H. W.; Zhang, Y.; Wang, L.; Xu, B. *Chemical Communications* **2004**, 208-209.
46. Adams, D. J.; Mullen, L. M.; Berta, M.; Chen, L.; Frith, W. J. *Soft Matter* **2010**, *6*, 1971-1980.
47. Adams, D. J.; Butler, M. F.; Frith, W. J.; Kirkland, M.; Mullen, L.; Sanderson, P. *Soft Matter* **2009**, *5*, 1856-1862.
48. Xu, H. X.; Das, A. K.; Horie, M.; Shaik, M. S.; Smith, A. M.; Luo, Y.; Lu, X. F.; Collins, R.; Liem, S. Y.; Song, A. M.; Popelier, P. L. A.; Turner, M. L.; Xiao, P.; Kinloch, I. A.; Ulijn, R. V. *Nanoscale* **2010**, *2*, 960-966.
49. Cheng, G.; Castelletto, V.; Moulton, C. M.; Newby, G. E.; Hamley, I. W. *Langmuir* **2010**, *26*, 4990-4998.
50. Chen, L.; Revel, S.; Morris, K.; Serpell, L. C.; Adams, D. J. *Langmuir* **2010**, *26*, 13466-13471.
51. Nanda, J.; Banerjee, A. *Soft Matter* **2012**, *8*, 3380-3386.
52. Liang, G. L.; Yang, Z. M.; Zhang, R. J.; Li, L. H.; Fan, Y. J.; Kuang, Y.; Gao, Y.; Wang, T.; Lu, W. W.; Xu, B. *Langmuir* **2009**, *25*, 8419-8422.
53. Gupta, M.; Bagaria, A.; Mishra, A.; Mathur, P.; Basu, A.; Ramakumar, S.; Chauhan, V. S. *Advanced Materials* **2007**, *19*, 858-+.

54. Rajashankar, K. R.; Ramakumar, S.; Mal, T. K.; Chauhan, V. S. *Angewandte Chemie-International Edition in English* **1994**, *33*, 970-973.
55. Ramagopal, U. A.; Ramakumar, S.; Sahal, D.; Chauhan, V. S. *Proceedings of the National Academy of Sciences of the United States of America* **2001**, *98*, 870-874.
56. Lisowski, M.; Jaremko, +.; Jaremko, M.; Mazur, A.; Latajka, R.; Makowski, M. *Biopolymers* **2010**, *93*, 1055-1064.
57. Ryu, J. H.; Lee, Y. H.; Kong, W. H.; Kim, T. G.; Park, T. G. *Journal of Controlled Release* **2011**, *152*, E236-E237.
58. Estroff, L. A.; Hamilton, A. D. *Chemical Reviews* **2004**, *104*, 1201-1217.
59. Makarevic, J.; Jokic, M.; Peric, B.; Tomisic, V.; Kojic-Prodic, B.; Zinic, M. *Chemistry-A European Journal* **2001**, *7*, 3328-3341.
60. Iwaura, R.; Yoshida, K.; Masuda, M.; Ohnishi-Kameyama, M.; Yoshida, M.; Shimizu, T. *Angewandte Chemie-International Edition* **2003**, *42*, 1009-+.
61. Shimizu, T.; Kogiso, M.; Masuda, M. *Journal of the American Chemical Society* **1997**, *119*, 6209-6210.
62. Kogiso, M.; Ohnishi, S.; Yase, K.; Masuda, M.; Shimizu, T. *Langmuir* **1998**, *14*, 4978-4986.
63. Doan, V.; Koppe, R.; Kasai, P. H. *Journal of the American Chemical Society* **1997**, *119*, 9810-9815.
64. Hanabusa, K.; Hirata, T.; Inoue, D.; Kimura, I.; Shirai, H. *Colloids and Surfaces A-Physicochemical and Engineering Aspects* **2000**, *169*, 307-315.
65. Reddy, A.; Sharma, A.; Srivastava, A. *Chemistry-A European Journal* **2012**, *18*, 7575-7581.
66. Maitra, U.; Mukhopadhyay, S.; Sarkar, A.; Rao, P.; Indi, S. S. *Angewandte Chemie-International Edition* **2001**, *40*, 2281-+.
67. Toyama, B. H.; Weissman, J. S. *Annual Review of Biochemistry, Vol 80* **2011**, *80*, 557-585.
68. Perczel, A.; Park, K.; Fasman, G. D. *Proteins-Structure Function and Genetics* **1992**, *13*, 57-69.
69. Whitmore, L.; Wallace, B. A. *Biopolymers* **2008**, *89*, 392-400.
70. (a) Gregoire, S.; Irwin, J.; Kwon, I. *Korean Journal of Chemical Engineering* **2012**, *29*, 693-702; (b) Greenfield, N. J. *Nature Protocols* **2006**, *1*, 2527-2535; (c) Kelly, S. M.,. Price, N. C. *Current Protein and Peptide Science*, 2000, 1, 349-384.
71. Greenfield, N. *Current Contents/Life Sciences* **1982**, 28.
72. Morris, K.; Serpell, L. *Chemical Society Reviews* **2010**, *39*, 3445-3453.
73. Goldschmidt, L.; Teng, P. K.; Riek, R.; Eisenberg, D. *Proceedings of the National Academy of Sciences of the United States of America* **2010**, *107*, 3487-3492.
74. Hirst, A. R.; Coates, I. A.; Boucheteau, T. R.; Miravet, J. F.; Escuder, B.; Castelletto, V.; Hamley, I. W.; Smith, D. K. *Journal of the American Chemical Society* **2008**, *130*, 9113-9121.
75. Escuder, B.; LLusar, M.; Miravet, J. F. *J.Org.Chem.* **2006**, *71*, 7747-7752.
76. Tycko, R. *Quarterly Reviews of Biophysics* **2006**, *39*, 1-55.
77. Paravastu, A. K.; Leapman, R. D.; Yau, W. M.; Tycko, R. *Proceedings of the National Academy of Sciences of the United States of America* **2008**, *105*, 18349-18354.

78. Mehta, A. K.; Lu, K.; Childers, W. S.; Liang, Y.; Dublin, S. N.; Dong, J. J.; Snyder, J. P.; Pingali, S. V.; Thiyagarajan, P.; Lynn, D. G. *Journal of the American Chemical Society* **2008**, *130*, 9829-9835.
79. Liang, Y.; Pingali, S. V.; Jogalekar, A. S.; Snyder, J. P.; Thiyagarajan, P.; Lynn, D. G. *Biochemistry* **2008**, *47*, 10018-10026.
80. Challis, B. C.; Bartlett, C. D. *Nature* **1975**, *254*, 532-533.
81. Jung, G. *Angewandte Chemie-International Edition in English* **1991**, *30*, 1051-1068.
82. Barbaste, M.; Rolland-Fulcrand, V.; Roumestant, M. L.; Viallefont, P.; Martinez, J. *Tetrahedron Letters* **1998**, *39*, 6287-6290.
83. Ferreira, P. M. T.; Maia, H. L. S.; Monteiro, L. S. *Tetrahedron Letters* **1999**, *40*, 4099-4102.
84. Wieland, T.; Ohnacker, G.; Ziegler, W. *Chemische Berichte-Recueil* **1957**, *90*, 194-201.
85. Schmidt, U.; Lieberknecht, A.; Wild, J. *Synthesis-Stuttgart* **1988**, 159-172.
86. Nakagawa, Y.; Nakajima, K.; Okawa, K.; Tsuno, T.; Iwai, M.; Kawai, H. *Bulletin of the Chemical Society of Japan* **1972**, *45*, 1162-&.
87. Sommerfeld, T. L.; Seebach, D. *Helvetica Chimica Acta* **1993**, *76*, 1702-1714.
88. Ferreira, P. M. T.; Monteiro, L. S.; Pereira, G.; Ribeiro, L.; Sacramento, J.; Silva, L. *European Journal of Organic Chemistry* **2007**, 5934-5949.
89. Pennycook S.J., Lupini A.R., Varela M., Borisevich A.Y., Peng Y., Oxley M.P., van Benthem K., and Chisholm M.F. Scanning transmission electron microscopy for nanostructure characterization. Scanning microscopy for nanotechnology: techniques and applications [Chapter 6], 152-191. 2007. New York, NY, Springer.
90. Reches, M.; Gazit, E. *Nano Letters* **2004**, *4*, 581-585.
91. Vauthey, S.; Santoso, S.; Gong, H. Y.; Watson, N.; Zhang, S. G. *Proceedings of the National Academy of Sciences of the United States of America* **2002**, *99*, 5355-5360.
92. Song, Y. J.; Challa, S. R.; Medforth, C. J.; Qiu, Y.; Watt, R. K.; Pena, D.; Miller, J. E.; van Swol, F.; Shelnutt, J. A. *Chemical Communications* **2004**, 1044-1045.
93. Vogel, A.I.; Tatchell, A.R., Furnis B.S.; Hannaford, A.J.; Smith, P.W.G. Vogel's Textbook of Practical Organic Chemistry, 5th. London, Longman Group UK Limited.
94. Yan, X. H.; He, Q.; Wang, K. W.; Duan, L.; Cui, Y.; Li, J. B. *Angewandte Chemie-International Edition* **2007**, *46*, 2431-2434.